Mon. Not. R. Astron. Soc. **368,** 121–140 (2006) doi:10.1111/j.1365-2966.2006.10095.x

Runaway collisions in young star clusters – I. Methods and tests

Marc Freitag,[1,2]★† Frederic A. Rasio[2] and Holger Baumgardt[3]

[1]*Astronomisches Rechen-Institut, Mönchhofstrasse 12-14, D-69120 Heidelberg, Germany*
[2]*Department of Physics and Astronomy, Northwestern University, Evanston, IL 60208, USA*
[3]*Sternwarte, Universität Bonn, Auf dem Hügel 71, 53121 Bonn, Germany*

Accepted 2006 January 18. Received 2006 January 16; in original form 2005 March 6

ABSTRACT

We present the methods and preparatory work for our study of the collisional runaway scenario to form a very massive star (VMS, $M_* > 400\,\mathrm{M}_\odot$) at the centre of a young, compact stellar cluster. In the first phase of the process, a very dense central core of massive stars ($M_* \simeq 30$–$120\,\mathrm{M}_\odot$) forms through mass segregation and gravothermal collapse. This leads to a collisional stage, likely to result in the formation of a VMS (itself a possible progenitor for an intermediate-mass black hole) through a runaway sequence of mergers between the massive stars. In this paper, we present the runaway scenario in a general astrophysical context. We then explain the numerical method used to investigate it. Our approach is based on a Monte Carlo code to simulate the stellar dynamics of spherical star clusters, using a very large number of particles (a few 10^5 to several 10^6). Finally, we report on test computations carried out to ensure that our implementation of the important physics is sound. In a second paper, we present results from more than 100 cluster simulations realized to determine the conditions leading to the collisional formation of a VMS and the characteristics of the runaway sequences.

Key words: stellar dynamics – methods: N-body simulations – stars: formation – galaxies: nuclei – galaxies: starburst – galaxies: star clusters.

1 INTRODUCTION

Runaway collisions and mergers of massive stars following gravothermal contraction and core collapse in a young, dense star cluster provides a natural path to the formation of a massive object at the centre of the system (Ebisuzaki et al. 2001; Portegies Zwart & McMillan 2002; Gürkan, Freitag & Rasio 2004, hereafter GFR04). The basic idea goes back to the earliest studies of the quasar/active galactic nucleus (AGN) phenomenon (e.g. Spitzer & Saslaw 1966; Colgate 1967; Sanders 1970).

Runaways could easily occur in a variety of observed young star clusters such as the 'young populous clusters' (like the Arches and Quintuplet clusters near our Galactic Centre) and the 'super star clusters' found in all starburst environments, including most galactic mergers (Figer, McLean & Morris 1999; Gallagher & Smith 1999). The Pistol Star observed in the Quintuplet cluster (Figer et al. 1998) may well be the product of such a runaway, as demonstrated by direct N-body simulations (Portegies Zwart & McMillan 2002). If the massive runaway collision product collapses to a black hole (BH), this scenario also provides a route to the formation of intermediate-mass black holes (IMBHs) in star clusters. Dynamical evidence for IMBHs at the centres of some globular clusters has been reported for many years (Gebhardt, Rich & Ho 2002; Gerssen et al. 2002; van der Marel et al. 2002). Tentative evidence has also been reported for an IMBH in the Galactic Centre source IRS 13, which was recently resolved into a small cluster of bright stars (Maillard et al. 2004). This could be the remnant of a much larger cluster that got tidally disrupted as its orbit around the Galactic Centre decayed through dynamical friction (Hansen & Milosavljević 2003; Gürkan & Rasio 2005). The very bright ultraluminous X-ray source (ULX) associated with the young star cluster MGG 11 in the starburst galaxy M82 could also have been produced through runaway collisions (Portegies Zwart et al. 2004). A similar process may be responsible for the formation of IMBHs in larger clusters, such as proto-globular clusters, as well as seed BHs in proto-galactic nuclei. These can later grow through a variety of processes including gas accretion, stellar captures, and mergers (Murphy, Cohn & Durisen 1991; Freitag & Benz 2002b; Yu & Tremaine 2002; Hansen & Milosavljević 2003; Wyithe & Loeb 2003; Blandford 2004).

The questions we address here are also central to our understanding of low-frequency gravitational-wave (GW) sources and the development of data analysis and detection strategies for these sources. In addition, our work may be viewed as mainly relevant to galactic astronomy; the results could also have applications in extragalactic astronomy and cosmology. The direct injection into the centre of a galaxy of many IMBHs produced by collisional runaways in nearby young star clusters provides an important new channel

★Present address: Institute of Astronomy, University of Cambridge, Madingley Road, Cambridge CB3 0HA.
†E-mail: freitag@ast.cam.ac.uk

for building up the mass of a central supermassive BH through mergers (Portegies Zwart & McMillan 2002). It is possible that this process is still ongoing in our own Galactic Centre (Hansen & Milosavljević 2003; Kim, Figer & Morris 2004; Gürkan & Rasio 2005). In contrast, minor mergers of galaxies are unlikely to produce BH mergers, as the smaller BH will rarely experience enough dynamical friction to spiral in all the way to the centre of the more massive galaxy (Volonteri, Haardt & Madau 2003). These ideas are also of critical importance for the design and planning of the Laser Interferometer Space Antenna (LISA), since the inspiral of an IMBH into a massive black hole (MBH) provides one of the best sources of low-frequency GWs for the direct study of strong field gravity with a space-based interferometer (Cutler & Thorne 2002; Phinney 2003; Collins & Hughes 2004; Miller 2005). Although the SMBHs found in bright quasars and many nearby galactic nuclei are thought to have grown mainly by gas accretion (e.g. Sołtan 1982; Haehnelt, Natarajan & Rees 1998; Fabian & Iwasawa 1999; Richstone 2004), current models suggest that LISA will probe most efficiently a cosmological MBH population of lower mass, which is largely undetected (Menou 2003). LISA will measure their masses with exquisite accuracy, and their mass spectrum will constrain formation scenarios for high-redshift, low-mass galaxies and, more generally, hierarchical models of galaxy formation (e.g. Haehnelt & Kauffmann 2002; Hughes & Holz 2003; Volonteri et al. 2003; Sesana et al. 2004).

GFR04 concentrated on the early dynamical evolution of young, dense star clusters. They performed dynamical Monte Carlo (MC) simulations for systems containing up to 10^7 stars, and followed the rapid mass segregation of massive main-sequence (MS) stars and the development of the Spitzer instability. They showed that, with a realistic initial mass function (IMF), these systems can evolve to core collapse in a small fraction of the initial half-mass relaxation time. If the core-collapse time is less than the lifetime of the most massive MS stars, all stars in the collapsing core may then undergo runaway collisions. The study in GFR04 was limited to the first step in this process, up to the occurrence of core collapse. About 100 simulations were performed for clusters with a wide variety of initial conditions, varying systematically the cluster density profile, stellar IMF, and the number of stars. GFR04's results confirmed that, for clusters with a moderate initial central concentration and any realistic IMF, the ratio of core-collapse time to initial half-mass relaxation time is typically $\sim$0.1, in agreement with previous calculations. It was also found that, for all realistic initial conditions, the mass of the collapsing core (at the onset of collapse) is always close to $\sim 10^{-3}$ of the total cluster mass, very similar to the observed correlation between central BH mass and total cluster mass in a variety of environments (Magorrian et al. 1998; Merritt & Ferrarese 2001; Häring & Rix 2004).

In this and a following paper (Freitag, Gürkan & Rasio 2005, hereafter Paper II), we go a step further in our study of runaways, by modelling the actual stellar collisions and following the early growth of the massive runaway product.

This paper is organized as follows. In Section 2, we explain in more detail the scenario for forming a massive object through runaway collisions and review the previous works on the subject. In Section 3, we present the numerical method and physical ingredients used in our simulations. Test simulations are presented in Section 4. Finally, in Section 5, we summarize these results and introduce Paper II. In the latter, we will present the results of more than 100 simulations carried out to study runaway collisions in a variety of clusters.

2 THE COLLISIONAL RUNAWAY ROUTE

2.1 Important quantities

Before reviewing the collisional runaway scenario, it is useful to define some quantities which are often referred to.

If a star with mass M_1 and radius R_1 travels with relative velocity $V_{\rm rel}^{\infty}$ across a field of stars of mass M_2 and radius R_2 and number density n_2, the collision probability per unit time for this star, that is, the reciprocal of its collision time, is

$$\frac{1}{t_{\rm coll}^{(1,2)}} = S_{\rm coll} V_{\rm rel}^{\infty} n_2 \ \text{with}$$
$$S_{\rm coll} = \pi (R_1 + R_2)^2 \left[1 + \frac{2G(M_1 + M_2)}{(R_1 + R_2)(V_{\rm rel}^{\infty})^2} \right]. \quad (1)$$

An important velocity scale for collisions between such stars is given by

$$V_*^2 = 2G \frac{M_1 + M_2}{R_1 + R_2} = (617.5\,{\rm km\,s^{-1}})^2 \frac{M_1 + M_2}{{\rm M}_\odot} \frac{{\rm R}_\odot}{R_1 + R_2}. \quad (2)$$

In most situations, $V_{\rm rel}^{\infty} \ll V_*$ and the collision cross-section is dominated by gravitational focusing, $S_{\rm coll} \simeq 2\pi G(M_1 + M_2)(R_1 + R_2)$. In a system where all stars have mass M_*, radius R_*, density n and a Maxwellian velocity distribution with 1D velocity dispersion $\sigma_{\rm v}$ ($\ll V_*$), the collision time (after which, each star, on average, would have experienced one collision) is then (Binney & Tremaine 1987, equation 8–125)

$$t_{\rm coll} \simeq 2.1 \times 10^{12}\,{\rm yr} \frac{10^6\,{\rm pc^{-3}}}{n} \frac{\sigma_{\rm v}}{30\,{\rm km\,s^{-1}}} \frac{{\rm R}_\odot}{R_*} \frac{{\rm M}_\odot}{M_*}. \quad (3)$$

Two-body relaxation plays a central role in the evolution of most clusters considered here. The local relaxation time is (Spitzer 1987)

$$t_{\rm rlx} = 0.339 \frac{\sigma_{\rm v}^3}{G^2 \ln(\gamma_{\rm c} N_*)\, n \langle M_* \rangle^2} \simeq 4.8 \times 10^7\,{\rm yr} \times \frac{10}{\ln(\gamma_{\rm c} N_*)} \left(\frac{\sigma_{\rm v}}{30\,{\rm km\,s^{-1}}} \right)^3 \frac{10^6\,{\rm pc^{-3}}}{n} \left(\frac{\langle M_* \rangle}{{\rm M}_\odot} \right)^{-2}, \quad (4)$$

where $\langle M_* \rangle$ is the average stellar mass and N_* the total number of stars. For systems with a broad stellar mass spectrum, we use $\gamma_{\rm c} = 0.01$ in the Coulomb logarithm (see Section 4.2.1). The relaxation time defined this way only has a direct meaning for a single-mass population. In case of a mass spectrum, it serves as a reference time but relaxational evolution may (and does) happen on a small fraction of $t_{\rm rlx}$.

The core of a cluster is the central region where density and velocity dispersion are approximately constant. We use the definition of Spitzer (1987, equation 1–34) for the core radius,

$$R_{\rm core} = \left[\frac{9\sigma_{\rm v,c}^2}{(4\pi G \rho_{\rm c})} \right]^{1/2}, \quad (5)$$

where $\rho = \langle M_* \rangle n$ and underscore 'c' indicates central values.

2.2 Basic scenario: summary and expectations

For the reader's convenience, we summarize here the collisional runaway scenario presented in GFR04 for the formation of an IMBH

($100 < M_{\rm BH} < 10^5\,{\rm M}_\odot$) at the centre of a dense stellar cluster. In the next subsection, we briefly review previous works that have led to the formulation of this scenario or have pioneered its investigation.

The basic idea is to create, through a sequence of collisions, a stellar object much more massive than what normal star formation can produce, with mass of a few hundreds to a few thousands $\rm M_\odot$. We refer to these objects as 'very massive star' (VMS). If such a star does not lose too much of its mass to winds by the time it reaches the end of its life, it is likely to undergo complete collapse into a BH, without mass ejection (Fryer & Kalogera 2001; Heger et al. 2003), hence producing an IMBH.

Stellar collisions are extremely rare in most astrophysical environments. They can only play a role in systems with a high stellar density such as self-gravitating dense clusters. When the most massive stars initially present in a cluster explode as supernovae, the cluster expands significantly as a result of the mass loss and collisions stop (if they were ever occurring). Therefore, the formation of a VMS has to occur before massive stars evolve off the MS (including the giant phase would only make a small difference), that is, for a cluster containing stars up to $\sim$100 $\rm M_\odot$, within a few million years. It is possible that a cluster could be *born* in a collisional state, that is, with an average collision time shorter than this, so that it would have been even more collisional while its stars were still on the pre-MS. This has been discussed as a way of creating all stars more massive than $\sim$10 $\rm M_\odot$ (Bonnell, Bate & Zinnecker 1998; Bally & Zinnecker 2005, and references therein). However, we focus here on the simpler case of a gas-free cluster with all stars on the MS initially.

Two-body relaxation provides a mechanism to increase the central density of a cluster and possibly drive it to a collisional state. Although this process of gravothermal core contraction, eventually leading to core collapse, also operates in single-mass clusters, it is much more important for realistic clusters with a broad IMF. The most massive stars will then be subject to dynamical friction and drift to the centre. In all realistic cases, the cluster encounters the Spitzer instability, meaning that this *mass-segregation* process leads to the formation of central core of massive stars that decouples as a self-gravitating system before the most massive stars can achieve energy equipartition with lighter objects. The system of massive stars then experiences core collapse on its own, very short, timescale. The high concentration of massive stars at the centre of the cluster eventually leads to a high collision rate.

The process of rapid mass segregation and core collapse in clusters with a broad IMF was the subject of GFR04. There, the relaxation-driven evolution of clusters with a variety of structures and IMF was followed. A key finding of this work is that for a given cluster structure but for all power-law mass spectra, $\mathrm{d}N_*/\mathrm{d}M_* \propto M_*^{-\alpha}$ with $\alpha \in [1.4, 3]$ as well as for Kroupa (Kroupa, Tout & Gilmore 1993) and Miller & Scalo (1979) IMFs, the core-collapse time $t_{\rm cc}$, expressed in units of the initial half-mass or central relaxation time [$t_{\rm rh}(0)$, $t_{\rm rc}(0)$, see GFR04] depends only on the ratio of the maximum to the average stellar mass, $\mu \equiv M_{*,\max}/\langle M_*\rangle$. Furthermore, for $\mu > 50$, a regime reached by all realistic IMFs, the dependency flattens to a constant $t_{\rm cc}/t_{\rm rh}(0) \simeq 0.07$–$0.08$ for Plummer models. Even more interestingly, this value, when expressed in units of $t_{\rm rc}(0)$, appears to be independent of the cluster's structure,[1] $t_{\rm cc}/t_{\rm rc}(0) \simeq 0.15$. GFR04 also found that, in contrast to core collapse in single-mass clusters, the mass of the contracting core, instead of decreasing to zero, reaches a finite value, representing in all cases a fraction of $(1.5$–$3)\times 10^{-3}$ of the total cluster mass.

These findings led us to the following two simple expectations.

(i) If the dynamical role of binaries can be neglected (see discussion in Appendix A), any cluster where the core-collapse time, $t_{\rm cc} \simeq 0.15\,t_{\rm rc}(0)$ (for realistically broad IMF) is shorter than the stellar evolution time of the most massive stars present, $t_* \simeq 3$ Myr (if the mass function extends to $\sim$100 $\rm M_\odot$) will enter a phase of rapid collisions between the massive stars that drive the core collapse. If the central velocity dispersion at that time is not in excess of $\sim$1000 km s^{-1}, collisions are not too disruptive and can lead to growth by mergers (Lai, Rasio & Shapiro 1993; Freitag & Benz 2005). Since the most massive object will have the largest cross-section for further collisions, it is expected to grow in a runaway fashion, that is, much faster than any other star (see the simple mathematical model in Section 2.3).

(ii) When a runaway occurs, the final mass attained by the central VMS cannot exceed about 3×10^{-3} of the total cluster mass. This is also in agreement with the mass of the final collision product formed in several previous N-body simulations of runaways (Portegies Zwart et al. 1999a; Portegies Zwart & McMillan 2002).

In Paper II, we put these expectations to the test through cluster simulations that include stellar collisions. We will see that, by and large, our results confirm point (i). For large cluster masses ($\gtrsim 10^7\,{\rm M}_\odot$), cluster evolution may be driven, from the beginning, by collisions, thus accelerating collapse so that runaway may happen at lower densities than predicted by (i). We do not find support in our simulations for the prediction (ii), likely, because our simulation method may not be able to predict correctly the final mass attained at the end of the runaway.

An obvious and legitimate question is whether the condition $t_{\rm cc} = t_* = 3$ Myr is ever fulfilled in real clusters. This is illustrated in Fig. 1 where we show this condition for a variety of King models in a plane representing the (initial) mass $M_{\rm cl}(0)$ and half-mass radius $R_{\rm h}(0)$ of the cluster. We have assumed a 0.2–120 $\rm M_\odot$ Salpeter IMF ($\langle m\rangle \simeq 0.69\,{\rm M}_\odot$, $\mu \simeq 174$). We chose $M_{\rm cl}(0)$ and $R_{\rm h}(0)$ as parameters because their present-day values are more easily accessible to observation than, say, the central density, and because they probably vary less than other quantities during cluster evolution. On the other hand, these quantities do not by themselves determine $t_{\rm rc}(0)$ and, hence, $t_{\rm cc}$; one needs to know how concentrated the cluster was initially (as measured, for instance, by the ratio of core radius to half-mass radius), a piece of information very poorly constrained by observations of evolved clusters. For the sake of simplicity, we restrict our discussion to the King family of cluster models, for which increasing W_0 corresponds to increasing concentration. We note that, although most numerical simulations so far have been done with moderate initial concentration, $W_0 \leqslant 6$, observations of young clusters suggest they may initially have very small cores, corresponding to $W_0 \geqslant 8$ (Campbell et al. 1992; Moffat, Drissen & Shara 1994; but see McCrady, Gilbert & Graham 2003, concerning the core radius of R136). For initial W_0 values ranging from 1 to 12, we have plotted the line indicating clusters with $t_{\rm cc} = 0.15\,t_{\rm rc}(0) = t_* = 3$ Myr. Below the line, a cluster with that W_0 would have shorter $t_{\rm cc}$. Points of various shapes denote observed clusters (young or old; see caption). We see that, even for a relatively moderate $W_0 = 7$, a few clusters inhabit the region of parameter space for which one expects fast core collapse, possibly leading to collisional runaway.

There is an important caveat to be made, concerning the interpretation of the results of GFR04 and Fig. 1. For a 0.2–120 $\rm M_\odot$ Salpeter IMF, only a fraction of $\sim 4 \times 10^{-4}$ of the stars are more massive

[1] Provided one can define a non-zero $t_{\rm rc}(0)$, which is not the case for γ-models with $\gamma < 2$ (Dehnen 1993; Tremaine et al. 1994).

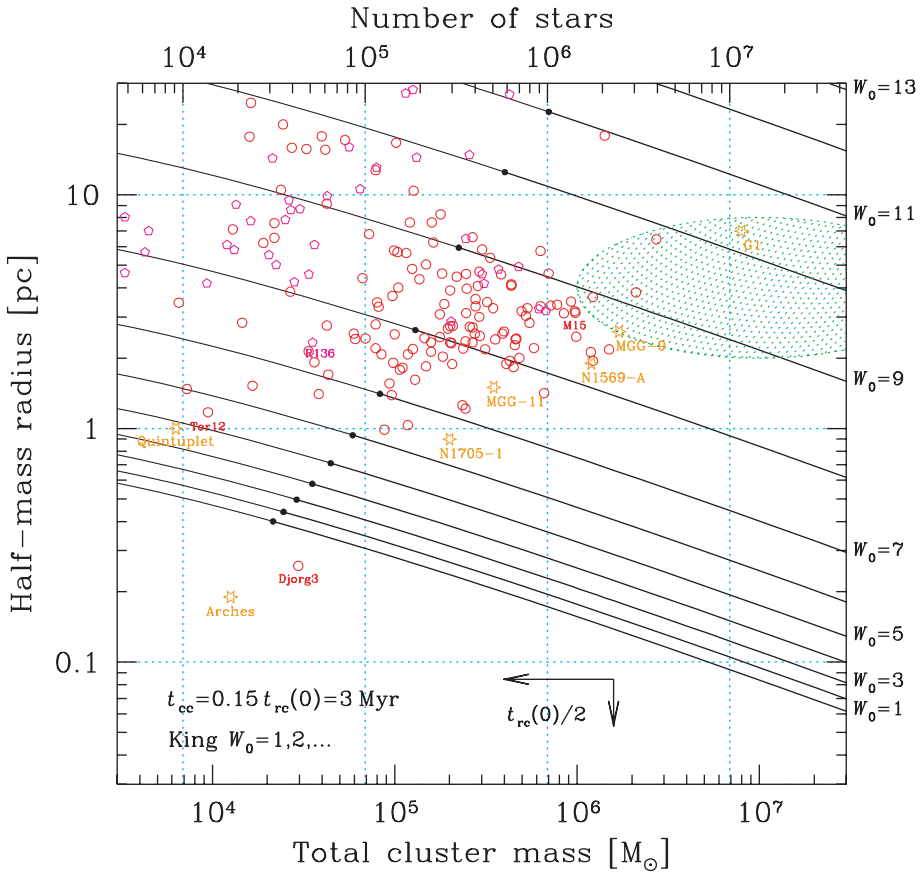

Figure 1. Conditions for rapid core collapse. This diagram shows which cluster masses, radii and initial concentrations will lead to core collapse in less than 3 Myr, that is, before the most massive stars evolve off the MS (a necessary condition for collisional runaway to occur). We consider clusters that have initially the structure of King models, with various concentrations, parametrized by the dimensionless central potential, W_0. The IMF is assumed to be Salpeter between 0.2 and 120 $M_\odot$ ($\langle M_* \rangle \simeq 0.69\,M_\odot$). In GFR04 we have showed that, for this or other similar IMF, core collapse occurs in $0.15\,t_{\rm rc}(0)$, independent of W_0. Each solid line corresponds to the condition $t_{\rm cc} = 3$ Myr for a given value of W_0 (see labels on the right-hand side of the frame). Below this line, the core-collapse time is shorter, above, it is longer. The dots on the lines correspond to models with 10 000 stars in their (initial) core. For this IMF, only a fraction of $\sim 4 \times 10^{-4}$ of the stars are more massive than 50 $M_\odot$, corresponding to approximately 4 such stars in the core. The arrows show how much of a decrease in the total mass $M_{\rm cl}$ or half-mass radius $R_{\rm h}$ leads to a shortening of $t_{\rm cc}$ by a factor of 2. We also show the position in the ($M_{\rm cl}$, $R_{\rm h}$) plane of a variety of observed clusters. The circles (in red in the online color version) are the Milky Way globular clusters from the compilation by Harris (1996, updated online at http://physun.physics.mcmaster.ca/Globular.html); the (magenta) pentagons are Low Magellanic Cloud clusters (Mackey & Gilmore 2003). Stars (in orange) represent populous young clusters,'super star clusters' and the cluster G1 of M 31. Data for the Arches and Quintuplet clusters are taken from Figer (2004), for NGC 1705-1 and NGC 1569-A from Ho & Filippenko (1996) and for MGG-9 and MGG-11 (in M 82) from McCrady et al. (2003). The shaded ellipse (in green) is the region in which the nuclei of dwarf ellipticals and bulgeless spiral galaxies are observed (Geha, Guhathakurta & van der Marel 2002; Walcher et al. 2005). For MW globular clusters, an age of 10 Gyr was assumed and the total mass was increased to correct for the decrease of the stellar average mass due to evolution of massive stars (but no account has been made of tidal stripping of stars).

than 50 $M_\odot$. To have 10^4 stars with approximately four such massive stars within the core of a $W_0 = 3$ or 8 cluster, the total number of stars must be 4.2×10^4 or 1.9×10^5, respectively. These values are indicated, for the various W_0, as black dots on the corresponding curves of Fig. 1. Actually, our result that, for sufficiently large number of particles, the core collapse occurs on a given fraction (0.15) of the initial *central* relaxation time $t_{\rm rc}(0)$, does not necessarily imply that only massive stars initially in the core [where the relaxation time is $\approx t_{\rm rc}(0)$] are responsible for the process. If it were the case, $t_{\rm cc}$ would be of the order of the dynamical friction time-scale in the core, $t_{\rm df,c} \simeq \mu^{-1} t_{\rm rc}(0) \leqslant 0.02\,t_{\rm rc}(0)$ which is much shorter than the value we find. This indicates that massive stars initially outside the core have time to reach the centre.

2.3 Previous works on collisional runaway

Colgate (1967) was the first to discuss the possibility of forming stars much more massive than initially present in a dense cluster through a sequence of stellar collisions. He suggested this mechanism as a way to create a large population of massive stars in a galactic nucleus to explain the quasar luminosities through enhanced supernova rates. He pointed out that, provided the collisions always result in mergers with little mass loss, a runaway situation should ensue, with one star growing to a very large mass in a short time but also estimated that its growth would actually terminate at $\sim 50\,M_\odot$ because, assuming a $R_* \propto M_*$ relation, the runaway object would then become too diffuse to stop 1-$M_\odot$ impactors ('transparency' problem). A more realistic

mass–radius relation (*M–R* relation) for MS stars more massive than $\sim 30\,\mathrm{M}_\odot$ (see equation 12 below) actually corresponds to nearly constant projected mass density M_*/R_*^2 so that this argument does not apply if the growing star has time to contract back to normal MS structure between collisions.

Following Colgate (1967), one may gain some insight to the runaway mechanism by considering an idealized situation in which one star of mass $M(t)$ and radius $R(t)$ grows by merging (without mass loss) with stars of mass and radius, m and r. One assumes $M \gg m$ (and $R \gg r$) and a constant density n of light stars, with a (3D) velocity dispersion σ_3. Then, using equation (1), the growth rate of the massive star reads

$$\frac{\mathrm{d}M}{\mathrm{d}t} = \frac{m}{t_{\rm coll}} \simeq mn\sigma_3\,\pi(r+R)^2\left[1+\frac{2G(m+M)}{(r+R)\sigma_3^2}\right]$$
$$\simeq 2\pi G\sigma_3^{-1}nmMR = \frac{M_0}{t_0}\left(\frac{M}{M_0}\right)^{1+\beta},$$
$$\text{with } t_0^{-1} = 2\pi G\sigma_3^{-1}nmR_0. \qquad (6)$$

This holds for strong gravitational focusing and a power-law *M–R* relation, $R = R_0(M/M_0)^\beta$. The solution of this differential equation, for $M(t=0) = M_0$ is

$$M(t) = \frac{M_0}{[(m/M_0)(1-t/t_{\rm div})]^{1/\beta}} \text{ with } t_{\rm div} = \frac{t_0}{\beta}. \qquad (7)$$

Hence, in this toy model, M becomes formally infinite after a finite time $t_{\rm div}$, if the exponent β is positive. More detailed analysis of the evolution of the whole distribution of stellar masses through the use of the so-called 'coagulation equation' also leads to the condition $\beta > 0$ for runaway to be possible (Lee 1993, 2000; Malyshkin & Goodman 2001). This kind of approach, ignoring stellar dynamical effects as it does, can only serve as a preliminary guide. A rough estimate of $t_{\rm div}$ in a static cluster core would be

$$t_{\rm div} = \frac{\sigma_3}{2\pi\beta Gnm R_0} \approx \beta^{-1} t_{\rm dyn}\frac{R_{\rm c}}{R_0} \qquad (8)$$

where $t_{\rm dyn}$ is the core dynamical time. One sees that this is a very long time-scale because $R_{\rm c}/R_0$ is typically (much) larger than 10^6.

Sanders (1970) investigated the possibility of runaway collisions in dense galactic nuclei [without a central (I) MBH], using a more refined model than Colgate's. The evolution of a population of stars subject to collisions was followed using a 'particles-in-a-box' MC method. The outcome of the collisions (occurrence of merger, amount of mass and energy loss) was determined using a generalization of the semi-analytical method of Spitzer & Saslaw (1966). The structure and dynamics of the cluster were not resolved. Instead, the system was treated as homogeneous within a spherical domain, its size and density being evolved by considering the amount of mass and energy lost through evaporation of stars and collisions, respectively, and assuming permanent virial equilibrium. All the gas lost in collisions was recycled into stars. The velocities were picked from a Maxwellian distribution with equipartition between stars of various masses. Thanks to a shallower *M–R* relation with $\beta = 0.7$, there was no transparency saturation to the growth of a VMS, which was followed from $0.5\,\mathrm{M}_\odot$ to more than $300\,\mathrm{M}_\odot$ in a 10^7-$\mathrm{M}_\odot$ nucleus.[2] A cluster model 10 times more massive, with the same initial velocity dispersion of $\sim 500\,\mathrm{km\,s^{-1}}$, did not exhibit any sign of runaway because the velocity dispersion raised above $1000\,\mathrm{km\,s^{-1}}$ and thus collisions became disruptive.

Lightman & Shapiro (1978), citing unpublished work by Fall and Lightman, exposed the conditions for the onset of a collisional runaway using a simple evaporative analytical model for the contraction of the core of a single-mass globular cluster. They found that the core must evolve to a state containing only a few hundreds to thousands of stars with a velocity dispersion of the order of $200\,\mathrm{km\,s^{-1}}$, but such approach lacks physical ingredients such as mass segregation which is key in the evolution of more realistic systems. At any rate, an important point made in this work was that, in the collisional stage, the stars should experience mergers at such high a rate that they should have no time to recover thermal equilibrium between two collisions and could well stay bloated, hence bringing back the transparency problem. The famous paper of Begelman & Rees (1978) introduced the process of runaway collisions to a larger audience as 'one of the quickest routes to the formation of a massive object in a dense stellar system'. However, although they mentioned mass-segregation as a way to increase the density of massive stars on a shorter time-scale, a self-consistent picture of the evolution a cluster subject to relaxation and collisions was still missing.

Lee (1987) and Quinlan & Shapiro (1990) (hereafter QS90) were first to study the role of collisional mergers in numerical models self-consistently resolving the structure and evolution of stellar clusters (without a central MBH). They applied very similar simulation methods and assumptions to quite different systems. Using codes that solve the Fokker–Planck (FP) equation, they had to keep the stellar mass function discretized into 'components' and represented the cluster as a finite set of distribution functions (in energy-space), one for each stellar mass. This approach has the advantage of producing results virtually devoid of noise but imposes a very artificial treatment of stellar evolution and collisions. Stars in the same mass component have to share the exact same properties, including some average age updated as time passes and merger products are added to the components, a possible cause of rejuvenation because the authors assumed complete mixing of the stellar gas during collisions. Collisions were treated as mergers without any mass loss. The mass and orbital energy of mergers of any mass have to be cast into the predefined mass components. Another questionable aspect of FP simulations, when applied to collisional runaways, is the applicability of this formalism to mass components containing a very small number of stars (sometimes less than one). These models also included the dynamical formation of binaries through three-body interactions and their subsequent hardening (and ejection) as a central source of energy capable of reversing core collapse and turning off collisions in clusters with a relatively low number of stars. It

[2] Lightman & Shapiro (1978) have stated the transparency problem in the following way. The growing star will be unable to stop a smaller impactor when the latter has more kinetic energy (at infinity) than what is required to punch a hole of its own cross-section through the massive object, that is, to unbound the mass it sweeps by passing through it. Neglecting the central mass concentration of the star, this leads to the (very approximate) condition

$$\frac{M}{R^2}r^2\,\frac{GM}{R} \approx m\sigma_3^2,$$

where M and R are the mass and radius of the runaway object, m and r the typical values for impactors, and σ_3 their velocity dispersion. Assuming a power-law *M–R* relation $R_* \propto M_*^\beta$ this translates into the following relation for the 'saturation mass' of the runaway object,

$$M_{\rm max} \approx m\left(\frac{v_*^2}{\sigma_3^2}\right)^{1/(3\beta-2)}$$

with $v_*^2 = Gm/r$. A typical β value for MS stars (i.e. assuming the runaway object stays on the MS) is $\beta \simeq 0.5$ and, except for very massive and compact clusters, $\sigma_3 < 0.3v_* \approx 300\,\mathrm{km\,s^{-1}}$, so $M_{\rm max} > 100\,\mathrm{m}$.

has since been realized that there is a high probability for collisions to occur when these three-body binaries interact with other stars, leading to a very significant reduction of the heating they provide (Chernoff & Huang 1996; Fregeau et al. 2004).

Both Lee (1987) and QS90 started with clusters where all stars initially have the same mass (0.7 and 1 $M_\odot$, respectively). In the work of Lee (1987), who was studying globular cluster models, collisions are actually tidal captures assumed to lead to quick merger. He concentrated on cases for which there was no real runaway growth or significant speed-up of core collapse due to mass-segregation. In all models but one, the core collapse was reversed by heating due to three-body binaries or by mass loss due to stellar evolution of mergers. As stars more massive than 22.4 $M_\odot$ were not allowed, the simulation had to be stopped for the only case in which conditions for the runaway were met. Lee (1987) suggested that a 'typical' proto-galactic nucleus, with 10^8 stars and a half-mass radius of $\sim$0.4 pc, would be subject to the 'merger instability'. The goal of QS90 was explicitly to look for the onset of runaway collisions as a way to create a VMS and, eventually, a seed IMBH that could grow into an MBH ($M_{\rm BH} > 10^5\,M_\odot$) at the centre of a galactic nucleus, as suggested by Begelman & Rees (1978). The results of these simulations suggested that runaway collisions would occur, provided that the half-mass relaxation time is shorter than $\sim 10^8$ yr (to beat stellar evolution) and $N_* \geqslant 3 \times 10^6$ (to avoid binary heating). The authors stressed that, as a result of mass segregation, the rise in the central velocity during collapse is only moderate and collisions do not become disruptive. Although not very realistic, these early studies made plausible the idea that successive collisions and mergers of MS stars could lead to the formation of a $\sim 10^2$–$10^3\,M_\odot$ object.

Through direct N-body simulations of clusters containing 2000–65 000 stars, Portegies Zwart et al. (1999a) and Portegies Zwart & McMillan (2002) showed that, in such low-N_* systems, dynamically formed binaries, far from preventing collisions (by heating the cluster and reversing collapse), actually *enhance* them by increasing the effective cross-section. In these small systems, once the few massive stars have segregated to the centre, one of them will repeatedly form a binary with another star and later collide with its companion when an interaction with a third star increases the binary's eccentricity or induces a chaotic 'resonant' interaction. The growth of this star is ultimately stopped by stellar evolution, or by the dissolution of the cluster in the tidal field of the parent galaxy. Given the small number of stars in these simulations, the maximum mass of the collision product is only $\sim$200 $M_\odot$ when mass loss from stellar winds is negligible.

More recently, Portegies Zwart et al. (2004) have improved on these early N-body simulations, considering models for two young clusters in the galaxy M 82: MGG-9 and MGG-11 (McCrady et al. 2003). Most calculations for MGG-11 were performed with 131 072 particles ('128k'), assuming a Salpeter IMF ranging from 1 to 100 $M_\odot$; those for MGG-9 used the same IMF and about four times more particles, in agreement with a higher estimated mass. For two simulations of MGG-11, the record-breaking number of 585 000 particles was used in order to extend the IMF down to a more realistic 0.2 $M_\odot$ (Salpeter) and 0.1 $M_\odot$ (Kroupa). The initial conditions used were King models with dimensionless central potential ranging from $W_0 = 3$ to 15. The authors found runaway growth of a VMS in all highly concentrated clusters ($W_0 \geqslant 9$) with a half-mass dynamical friction time-scale for 100-$M_\odot$ stars shorter than 4 Myr. The mass reached was at least 800 $M_\odot$ and up to 2700 $M_\odot$ depending on the M–R relation. Incidentally, they noted that no reasonable model for MGG-9 complies with these conditions but that MGG-11 may be in the right domain and suggested this may explain why a ULX is (possibly) associated with the latter but not with the former. In contrast to what was found in smaller systems, for models with $>10^5$ particles (and without primordial binaries), a significant number of collisions (of the order of 25–30 per cent) involve only single stars. Portegies Zwart et al. (2004) also performed one (very computer-intensive) 128k simulation for MGG-11 with $W_0 = 12$ and 10 per cent primordial hard binaries and found a slight *increase* in the collision rate and final mass of the runaway object, suggesting that primordial binaries cannot prevent the runaway process by halting the core-collapse process. Whether this holds in general, in particular for initially less concentrated clusters has yet to be established, through, for example, a series of MC cluster simulations including primordial binaries (Fregeau et al. in preparation).

3 SIMULATION METHODS AND PHYSICAL INGREDIENTS

In the present work, we use a set of stellar dynamical simulations for collisional clusters to establish the conditions and manner under which a runaway occurs. Our basic numerical tool is an MC code similar to the one used for GFR04 but developed independently and presenting many differences in its structure. We describe this code briefly in Section 3.1. The reason for using this different code here is that it was originally written to study high-density galactic nuclei including the effects of stellar collisions. In Section 3.2, we explain our treatment of collisions and discuss various relevant aspects of their physics.

3.1 The Monte Carlo code for cluster dynamics

In the past few years, a new MC code, ME(SSY)**2 (for 'Monte Carlo Experiments with Spherically SYmmetric Stellar SYstems') has been developed to follow the long-term evolution of dense clusters, with an emphasis on galactic nuclei (Freitag 2001; Freitag & Benz 2001, 2002b). This code is based on the scheme first proposed by Hénon (1973) to simulate globular clusters but, in addition to relaxation, it also includes collisions, stellar evolution, and, optionally, tidal disruptions and captures of stars by a central MBH through emission of gravitational waves.

The MC technique assumes that the cluster is spherically symmetric and represents it as a set of particles, each of which may be considered as a homogeneous spherical shell of stars sharing the same orbital and stellar properties. Unlike the MC code used in GFR04, in the present implementation, the number of particles may be lower than the number of stars in the simulated cluster (but the number of stars per particle has to be the same for each particle). Another important assumption is that the system is always in dynamical equilibrium so that orbital time-scales need not be resolved and the natural time-step is a fraction of the relaxation (or collision) time. Instead of being determined by the integration of its orbit, the position of a particle (i.e. the radius R of the shell) is picked up at random, with an R probability density that reflects the time spent at R: $\mathrm{d}P/\mathrm{d}R \propto 1/V_{\rm r}(R)$ where $V_{\rm r}$ is the radial velocity. Unlike the code of GFR04, our scheme adopts time-steps that are some small fraction f of the *local* relaxation (or collision) time: $\delta t(R) \simeq f \min(T_{\rm rel}, T_{\rm coll})$ with f of the order of or smaller than 0.05.[3] Consequently, the central parts of the cluster, where evolution is faster, are updated much more frequently than the outer parts. At each step, a

[3] One also makes sure that the time-step is significantly shorter than any stellar evolution time (MS lifetime) for stars around R.

pair of neighbouring particles is selected randomly with probability $P_{\rm selec} \propto 1/\delta t(R)$. This ensures that a particle stays for an *average* time $\delta t(R)$ at R before being updated. Because particles are evolved one pair at a time and to ensure perfect energy conservation, the (spherical) potential produced by the collection of particles is represented by a binary-tree structure allowing the determination of both, its value at any given R and its update after modification of the position or mass of a particle in $\mathcal{O}(\ln N_{\rm p})$ operations, where $N_{\rm p}$ is the particle number.

The relaxation is treated as a diffusion process, with the classical Chandrasekhar theory (Chandrasekhar 1960; Binney & Tremaine 1987), similarly to what is done in the code used in GFR04. This treatment shares many assumptions with the methods that are based on integrating the FP equation directly. Unlike those methods, ours is based on particles and hence allows us to incorporate further physics more naturally, for example, a continuous mass spectrum and the inclusion of an anisotropic velocity distribution. The most important addition for the purposes of this paper is stellar collisions. Unlike diffusive relaxation, collisions cannot be treated as a continuous process but are individual events, each of which may importantly affect the orbit, the mass or the mere existence of a particle. When a pair is selected, one computes the collision probability between a star of the first particle and a star of the second,

$$P_{\rm coll} = S_{\rm coll} V_{\rm rel}^{\infty} n\, \delta t. \tag{9}$$

$S_{\rm coll}$ is given by equation (1) and is connected to the maximum impact parameter for collision, $S_{\rm coll} = \pi b_{\rm max}^2$. Note that the total local stellar density n enters the relation, not n_1 or n_2 (Freitag & Benz 2002b). A random number is picked from the interval [0, 1[with uniform probability. If it is smaller than $P_{\rm coll}$, a collision between the two particles has to be simulated.[4] The impact parameter is determined by $b = b_{\rm max}\sqrt{X}$, where X is another random number from the interval [0,1[. The other parameters specifying the collision, that is, M_1, M_2 and $V_{\rm rel}^{\infty}$ are already known from the particles' properties. The method for determining the outcome of the collisions is explained in the next section.

3.2 Stellar collisions and stellar evolution

In this section, we explain some important aspects of the 'stellar micro-physics' of great importance for the runaway scenario in more detail: the outcome of collisions, stellar evolution and the interplay between them. We explain how we deal with these questions in our code and what are the associated uncertainties.

3.2.1 General considerations about collisions

Consider a collision between stars of masses M_1, M_2, and radii R_1, R_2. At large separation, their relative velocity is $V_{\rm rel}^{\infty}$ and impact parameter b. If they were point masses, their trajectories would be hyperbolas with separation and velocity at periastron,

$$d_{\rm min} = b\,\frac{1}{x+\sqrt{1+x^2}}, \tag{10}$$

$$V_{\rm max} = V_{\rm rel}^{\infty}\left(x+\sqrt{1+x^2}\right), \tag{11}$$

with $x = \left(\frac{V_*}{V_{\rm rel}^{\infty}}\right)^2 \left(\frac{R_1+R_2}{2b}\right)$.

If one neglects tidal effects until the stars touch, the relative velocity at contact is $V_{\rm cont} = \sqrt{(V_{\rm rel}^{\infty})^2 + V_*^2}$. Because of gravitational focusing, $d_{\rm min}$ is a more useful parameter than b to describe how central a collision is.

For $V_{\rm rel}^{\infty} \ll V_*$, gravitational focusing is important, $S_{\rm coll} \simeq 2\pi(R_1+R_2)G(M_1 1 M_2)(V_{\rm rel}^{\infty})^{-2}$ and $\mathrm{d}P/\mathrm{d}(d_{\rm min}) = {\rm const}$, and most collisions result in merger with little mass loss, $\delta M/M < 0.1$ (Benz & Hills 1987, 1992; Lai et al. 1993; Lombardi et al. 2002; Sills et al. 2002; Freitag & Benz 2005). When $V_{\rm rel}^{\infty} \simeq$ few V_*, a regime probably only reached in galactic nuclei in the vicinity of an MBH, the cross-section is geometrical, $S_{\rm coll} \simeq \pi\,(R_1+R_2)^2$, most encounters have relatively large $d_{\rm min}(\mathrm{d}P/\mathrm{d}(d_{\rm min}) \propto d_{\rm min})$ and are 'fly-bys', that is, both stars survive and remain unbound. Only nearly head-on collisions are highly disruptive and may lead to destruction of the smaller star or both (Benz & Hills 1987, 1992; Lai et al. 1993; Freitag & Benz 2002a, 2005).

At low relative velocities, two stars can become bound to each other, that is, form a binary, through the dissipation of orbital energy in tides near periastron, even if $d_{\rm min} > R_1 + R_2$ (Fabian, Pringle & Rees 1975). For velocities typical of globular clusters (10–50 km s^{-1}), such tidal binaries form up to $d_{\rm min}/(R_1+R_2) \simeq$ 2–3 (Portegies Zwart & Meinen 1993; Kim & Lee 1999). Their evolution is still a subject of debate and may be very complex, but given the fact that they form with very small pericentre separation and that the stars should swell due to the conversion of tidally excited oscillations into heat (McMillan, McDermott & Taam 1987; Kumar & Goodman 1996; Podsiadlowski 1996), it seems likely that they will promptly merge. Consequently, we could try to account for tidal captures by increasing the effective stellar radii for collisions at low $V_{\rm rel}^{\infty}$ (Lee 1987), but for simplicity and to stay on the conservative side when testing the runaway scenario, we decided to neglect this effect and only account for genuine collisions with $d_{\rm min} < R_1 + R_2$.

3.2.2 Mass–radius relation

One may expect the M–R relation to play an important role in determining collision rates through its influence on the cross-section. Fig. 2 show various M–R relations from the literature. For stars between ∼0.8 and ∼150 $\mathrm{M}_\odot$, we plot the radius at the beginning, middle and end of the MS (Schaller et al. 1992; Charbonnel et al. 1999; Lejeune & Schaerer 2001).[5] In the present work, the behaviour of the M–R relation beyond $M_* = 100\,\mathrm{M}_\odot$ is of particular concern because, within our assumptions, this will set the size of the runaway collision products and may have bearing on growth and rejuvenation rates. Hence, this may determine when stellar evolution will terminate the growth and what mass the runaway star has attained at this stage. Unfortunately, the radius of a VMS ($M_* > 100\,\mathrm{M}_\odot$) is highly uncertain. Ishii et al. (1999) have shown that a VMS may develop a very extended envelope of very low density (see also Stothers & Chin 1997; Figer et al. 1998; Baraffe et al. 2001). Their 1000-$\mathrm{M}_\odot$, $Z = Z_\odot$ model, for instance, has $R_* = 3000\,\mathrm{R}_\odot$ on the zero-age main-sequence (ZAMS), but its envelope represents only 3 per cent of the stellar mass so it is reasonable to assume this extended atmosphere will play a negligible role in collisions. Furthermore, this

[4] If each particle represents $N_{\rm st}$ stars, $N_{\rm st}$ identical collisions are assumed to take place. In this way, one may apply the result of the collision (new velocities, stellar masses, ...) to the particles themselves. If the collision results in a merger, only one particle is retained in the simulation. If both stars are completely disrupted, both particles are removed.

[5] Data available at http://obswww.unige.ch/∼mowlavi/evol/stev_database.html.

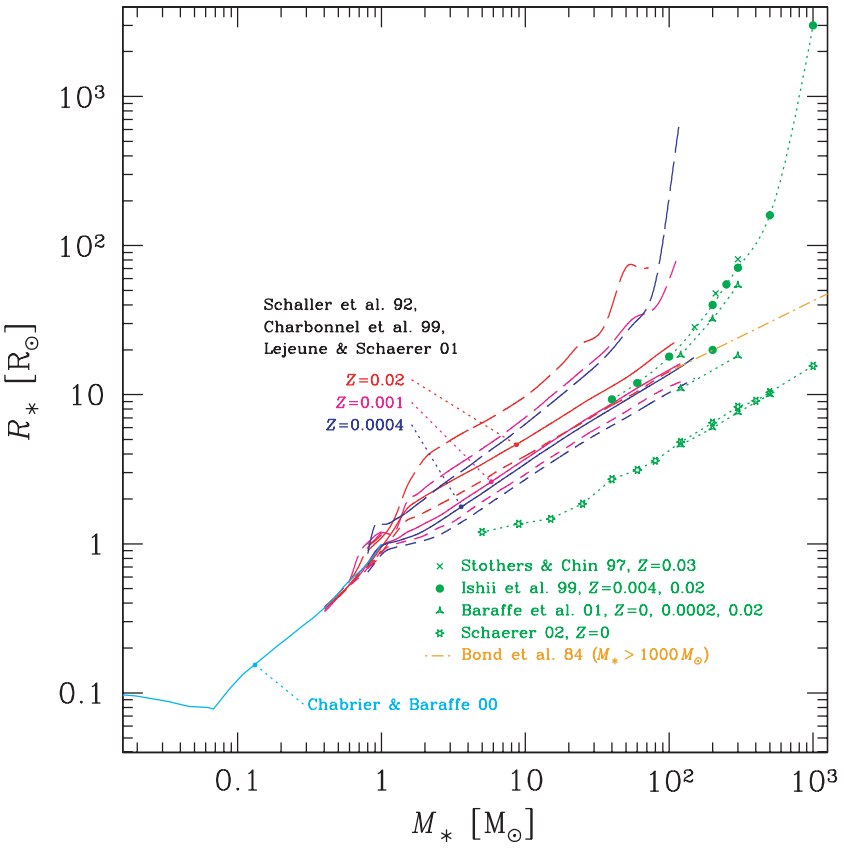

Figure 2. *M–R* relations for MS stars from various authors. The *M–R* for low masses (0.01–1 $M_\odot$, in cyan in the colour version) is from Fig. 3 of Chabrier & Baraffe (2000, $Z = Z_\odot = 0.02$, age of 5×10^9 yr) For intermediate masses, we plot radii from the Geneva stellar evolution group for three metallicities: $Z = 0.0004, 0.001, 0.02$ (in blue, magenta and red in the online color version of this figure) (Schaller et al. 1992; Charbonnel et al. 1999; Lejeune & Schaerer 2001). Short-dashed lines correspond to the ZAMS, solid lines to the radius when the star has lived half of its MS lifetime (or 5×10^9 yr for low-mass stars) and long-dashed lines to the end of the MS phase or at an age of 10^{10} yr at low masses. The maximum mass considered in these series of models is 100–150 $M_\odot$. All other *M–R* relations plotted here are for the ZAMS (Bond, Arnett & Carr 1984; Stothers & Chin 1997; Ishii, Ueno & Kato 1999; Baraffe, Heger & Woosley 2001; Schaerer 2002). Star with higher metallicity have larger radii. At $Z_\odot$, stars more massive than 100 $M_\odot$ have a huge diffuse envelope, due to metal opacity. The relation from Bond et al. (1984) [$R_* \simeq 1.6\,R_\odot\,(M_*/M_\odot)^{0.47}$] neglects this effect. It is established for $M_* \geqslant 10^4\,M_\odot$ but matches nearly perfectly the models for $M_* \geqslant 100\,M_\odot$.

structure is due to opacity from metals and is not present if the metallicity is low enough (Baraffe et al. 2001).

For the cluster simulations presented in this paper, we adopt a unique MS *M–R* relation constructed from $Z = 10^{-3}$ models from the following sources. For $M_*/M_\odot < 0.4$, we use fig. 3 of Chabrier & Baraffe (2000). For the ranges $0.4 \leqslant M_*/M_\odot < 1$ and $1 \leqslant M_*/M_\odot < 120$, we use models from Charbonnel et al. (1999) and Schaller et al. (1992), respectively. Finally, for stars more massive than 120 $M_\odot$, we apply a relation given by Bond et al. (1984),

$$R_* = 1.6\,R_\odot \left(\frac{M_*}{M_\odot}\right)^{0.47}. \qquad (12)$$

Even though this expression is for stars more massive than $10^4\,M_\odot$, it appears to match nicely with the *M–R* relation at $M_*/M_\odot < 120$, as shown in Fig. 2.

Focusing on low metallicity is reasonable: only if the metallicity is sufficiently low, is it clear that a VMS will be stable while on the MS (Baraffe et al. 2001),[6] that it will experience little evolutionary mass loss, and that it will collapse into a BH as a whole (Fryer & Kalogera 2001).

We do not account for the increase of the stellar radius during the MS evolution and use the size of the star at half its MS lifetime, or at an MS age of 5 Gyr for stars with MS lifetime exceeding 10 Gyr. Although it would be more consistent to let the stellar radii evolve, the extra complication involved in such an improvement is not justified in the face of the larger uncertainties introduced by other necessary simplifications, in particular concerning the size and evolution of collision products (see below). By the nature of the scenario studied here, we follow only the first few million years of the cluster evolution. Hence, low-mass stars should be given a size smaller than their 'half-MS' radius and closer to the ZAMS value. One can see in Fig. 2 that this only leads to a slight overestimate of the collision cross-sections which, being dominated by gravitational focusing, are proportional to the stellar radii. More important is the case of the most massive stars, say, $M_* > 50\,M_\odot$, which are expected to dominate the collisional process and may significantly evolve over

[6] But the question of the structure, stability and evolution of a VMS subject to a steady bombardment of smaller stars is another, unsettled question. Collapse to an IMBH may occur before the runaway collision product has evolved to thermal equilibrium, in which case the stability issues may be less relevant.

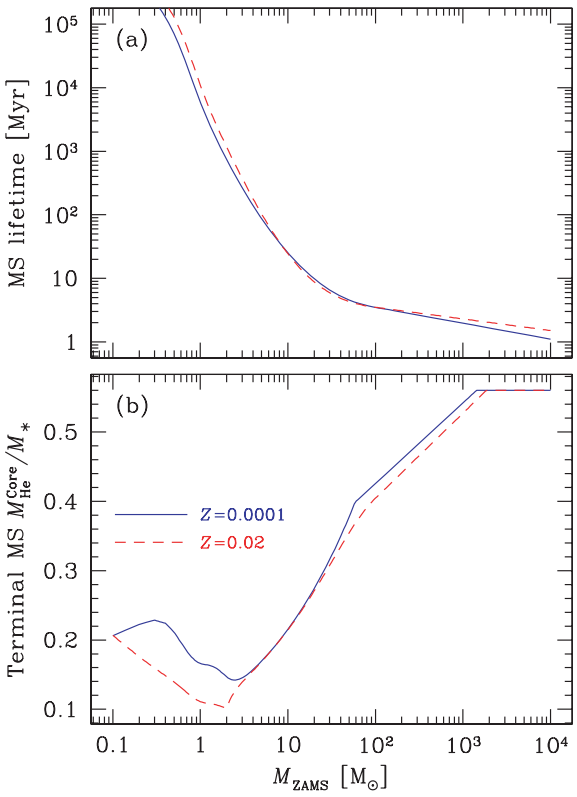

Figure 3. (a) MS lifetime for stars of various masses. (b) Relation between the mass of a MS star and the amount of helium produced in the core by hydrogen burning (at the terminal MS), expressed as a fraction of the total mass. Values for two metallicities are plotted. Data kindly provided by K. Belczynski. For masses larger than 120 $M_\odot$, extrapolation (linear in the quantities plotted) is used; the fractional amount of He produced is not allowed to exceed 0.56 (Bond et al. 1984).

the period of time considered here. Their size increases significantly during the late MS. Neglecting this may lead to an underestimate of their collision rates. A higher, possibly more realistic, size contrast between light and massive stars is likely to facilitate the runaway mechanism. However, by experimenting with large changes in the high-mass M–R relation, ranging from $R_* =$ constant to $R_* \propto M_*$, we have checked that this is of relatively little importance.

A more questionable simplification is to consider that all stars are initially on the MS. The runaway process has to start before the most massive stars in the IMF ($M_* \simeq 100\,M_\odot$) turn into compact remnants. This gives us at most 3 Myr (see Fig. 3a). This is to be compared with the duration of the pre-MS phase. After it has stopped accreting (and hence reached the 'birth-line'), a pre-MS star less massive than ∼6–8 $M_\odot$ is several times larger than on the ZAMS. The time required for contraction on to the ZAMS strongly increases with decreasing mass; it is shorter than 3 Myr only for stars more massive than 2–3 $M_\odot$ (Palla 2002). Consequently, in a young cluster, assuming for simplicity that accretion ceased for all stars at the same instant, low-mass stars are more extended and less dense than high-mass objects. During this phase their collision rate is higher than in the MS phase; however, their encounters with more massive but more compact stars may result in the tidal disruption of these low-mass objects rather than a 'clean' merger (Zinnecker & Bate 2002). We leave these complications out of our present study. We consider the models presented here as the simplest possible ones that incorporate all the key physical ingredients needed to investigate the runaway scenario. More sophistication could be included in further works, if deemed necessary.

3.2.3 *Collisional rejuvenation*

The stellar evolution of collision products has only been explored for the case of low-velocity mergers, relevant to globular clusters (Sills et al. 1997, 2001). Such encounters are only mildly supersonic and entropy is nearly conserved. Hence, the structure of the merger can be established by sorting the mass elements from the parent stars according to their entropy (Lombardi, Rasio & Shapiro 1995; Lombardi et al. 2002). The main uncertainty about the evolution of these objects is the mechanism, if any, responsible for decreasing the amount of angular momentum as the star relaxes to thermal equilibrium after the collision. For high-velocity collisions, significant dissipation occurs and entropy sorting is questionable, not to mention that, in most cases, both stars survive the collision unbound to each other ('fly-bys').

In view of these difficulties, we used a very simple procedure to set the stellar evolution of mergers, called *minimal rejuvenation*. We assume that, during a coalescence, the helium cores of both parent stars merge together, while the hydrogen envelopes combine to form the new envelope; no hydrogen is brought to the core. Furthermore, to assign an effective age to the merger, we assume that the mass of the helium core grows linearly with time during the MS and resort to stellar evolution models to provide the relation between the stellar mass and the helium core mass at the terminal age MS. This formalism is also applied to fly-bys during which part of the stellar envelopes is removed. In Fig. 3, we plot the MS lifetime and the total mass of helium produced during the MS phase as functions of the stellar mass (data provided by K. Belczynski; see Hurley, Pols & Tout 2000; Belczynski, Kalogera & Bulik 2002). For simplicity and because the dependence on metallicity is weak, we use the $Z = 10^{-4}$ data for all simulations. In any case, the thermal time-scale is always assumed to be shorter than the average time between collisions so that the MS M–R relation is applied to collision products. The validity of this hypothesis during the runaway growth of a massive star through repeated mergers is questionable and is discussed in Paper II (Section 2.2 in particular).

3.2.4 *Implementation and role of stellar evolution and mass loss*

ME(SSY)**2 implements a very simple prescription for stellar evolution (Freitag & Benz 2002b). While a star is on the MS, its mass and radius are kept constant. The duration of the MS, $T_{\rm MS}$, is given by detailed stellar models (Hurley et al. 2000). It is plotted for two metallicities in panel (a) of Fig. 3. For all simulations presented here, we use the data for metallicity $Z = 10^{-4}$, but it is obvious that the metallicity has little impact on $T_{\rm MS}$. On the other hand, the amount of mass loss on the MS increases strongly with Z (Vink, de Koter & Lamers 2001). While the possibility of runaway collisions in clusters with high metallicities, such as young populous or 'super' clusters observed in our and other galaxies is certainly of great interest; it is unlikely that a high-Z VMS will form an IMBH if it is left to evolve on the MS, precisely, because it should experience such high mass loss. Indeed, standard prescriptions for mass-loss rates indicate that stars more massive than ∼120 $M_\odot$ shed most of their mass on the MS if they are of solar metallicity. At $Z \simeq 4 \times 10^{-4}$, ∼120 $M_\odot$ stars lose only ∼10 per cent of their mass, but objects above ∼500 $M_\odot$ should evaporate themselves nearly completely (Lejeune & Schaerer 2001; Kudritzki 2002). Therefore, in

this work, we only consider (very) low metallicity. Also recall that, in GFR04, we studied whether mass loss on the MS could decrease the binding energy of the cluster enough to reverse core collapse and found that, even for solar metallicity, this only happens in a very small domain of the parameter space, namely for clusters with a core-collapse time already very close to the critical value of 3 Myr.

We assume that all mass lost by the stars is expelled from the cluster. This is probably a reasonable simplification for clusters with a relatively low escape velocity, like globular clusters but a poor one for (proto-)galactic nuclei in which a significant fraction of the gas could be retained. This approximation is discussed in Paper II.

In summary, for this work, the role of stellar evolution is only to set a clock against which core collapse and collisions have to race. When core collapse requires more time than the MS lifetime of massive stars, it will be terminated by SN mass loss (see fig. 13 of GFR04). This also holds for clusters of very low metallicities because all stars with mass between $\sim$8 and $\sim$40 $\mathrm{M}_\odot$ at the end of the nuclear burning phases should explode as supernovae, with considerable mass loss (Fryer & Kalogera 2001). Stellar evolution of a VMS interrupts the runaway collision sequence. If it turns into an IMBH, it may continue to grow, although presumably at a smaller rate, by tidally disrupting the MS stars while they still dominate the central density. When all normal MS stars more massive than about 20–25 $\mathrm{M}_\odot$ have turned into stellar BH with $M \gtrsim 10\,\mathrm{M}_\odot$, these objects will dominate the central region, expelling MS stars and thus quenching tidal disruptions. N-body simulations of systems with $N_* \leqslant 180\,000$ (Baumgardt, Makino & Ebisuzaki 2004a,b) have shown that the central IMBH will likely form a binary with a compact remnant which, although not compact enough to merge over a Hubble time through the emission of gravitational radiation, is probably very efficient at scattering off other stars, thus driving cluster re-expansion and preventing any significant growth of the IMBH. These conclusions presumably do not apply to systems containing 10^6 stars or more in which the binary should have a separation small enough for quick merging (Baumgardt et al. predict $a \propto M_{\mathrm{cl}}^{-0.95}$). Recent simulations performed with an MC code which incorporates primordial binaries have revealed the exciting possibility of the formation of two IMBHs. In models with more than 10 per cent primordial binaries, a first VMS starts growing at some distance from the centre through binary interactions, while the second forms in the centre, at the moment of core collapse through collision between single stars, as studied here (Gürkan, Fregeau & Rasio 2006).

The kind of MC code we use in this work does not include binary dynamics and, more generally, is not suited for following the cluster evolution when driven by a very small number of central objects. Hence, we do not attempt to study the evolution of the cluster and its central object once one VMS has formed and reached the end of its MS phase. This would be better studied using N-body methods to treat in detail the full dynamics of the central region.

3.2.5 Smoothed particle hydrodynamics collision simulations

In the MC method, collisions are handled on an event-by-event basis, rather than through average rates and outcomes as in FP codes. To treat collisions with as much realism as possible, we can use the results of 3D hydro simulations performed with the smoothed particle hydrodynamics (SPH) method (Benz 1990; Monaghan 1992; Rasio & Lombardi 1999). A set of some 14 000 SPH simulations of collisions between MS stars was performed by Freitag & Benz (2005). The original goal was to include the effects of collisions in stellar dynamical models of galactic nuclei (Freitag & Benz 2002b). This focus determined the parameter range covered in this study: stellar masses from $M_{\min} = 0.1\,\mathrm{M}_\odot$ to $M_{\max} = 74.3\,\mathrm{M}_\odot$, relative velocities in the range $V_{\mathrm{rel}}^\infty / V_* \simeq 0.03$–30 and impact parameter corresponding to $d_{\min}/(R_1 + R_2) = 0$–0.9. Because it proved intractable to summarize the outcome of these simulations (stellar masses, orbital energy and deflection angle) through a set of fitting formulae, we implemented a scheme to interpolate from SPH results in the 4D parameter space $(M_1, M_2, V_{\mathrm{rel}}^\infty, d_{\min})$. While this method proves adequate for galactic nuclei simulation in which velocities are high and it is therefore highly unlikely that mergers will lead to the formation of a star more massive than $M_{\max}$ (Freitag 2000; Freitag, Gürkan & Rasio 2004), it is not suited to the problem of runaway growth.

In most cluster simulations reported here and in Paper II, we simply assume that all collisions result in merger with no mass loss. We will see that this is a satisfying approximation because, in all but the most extreme cases, the central velocity dispersion is and remains relatively small. To go one step beyond this zeroth order 'sticky sphere' approximation and test its validity, for a subset of runs, we use the SPH results to allow for non-merging collisions and collisional mass loss in the way described below. For grazing collisions not resulting in a merger, we do not account for the reduction of the relative velocity or non-Keplerian deflection angle.

Complete disruption of both stars is extremely unlikely. Not only does it require a relative velocity of a few V_* but also a nearly head-on geometry. Hence, in this work, we consider only two possible outcomes: merger and 'fly-by'. Most low-velocity ($V_{\mathrm{rel}}^\infty < 0.1\,V_*$, say) encounters result in mergers but, in our SPH work, we have not studied those in much detail. Such collisions require a large amount of computation time because, unless the collision is nearly head-on, the pair does not merge immediately after first contact but forms a bound binary which goes through many successive periastron passages until final coalescence. In most cases, the hydrodynamical simulation was stopped before a merged star had formed. But it is very likely that any binary formed through a contact collision will eventually merge because the stars swell as their envelopes are shocked so that each pericentre passage is more dissipative. Hence, we can use our SPH results to establish the condition for merger. We have found the following parametrization to correctly predict the maximum merger impact parameter for all but a few SPH simulations:

$$\begin{aligned}\lambda_{\mathrm{merg}} &= c_0 + c_1 q + c_2 M_2 + c_3 l_{\mathrm{v}} + c_4 l_{\mathrm{v}} q + c_5 l_{\mathrm{v}} M_2 + \\ &\quad c_6 l_{\mathrm{v}}^2 + c_7 l_{\mathrm{v}}^2 q + c_8 l_{\mathrm{v}}^2 M_2, \\ \text{with } \lambda &= \frac{d_{\min}}{R_1^{(\mathrm{h})} + R_2^{(\mathrm{h})}},\quad q = M_1/M_2 \leqslant 1 \\ \text{and } l_{\mathrm{v}} &= \log_{10} \frac{V_{\mathrm{rel}}^\infty}{V_*^{(\mathrm{h})}},\quad V_*^{(\mathrm{h})} = \sqrt{\frac{2G(M_1+M_2)}{R_1^{(\mathrm{h})} + R_2^{(\mathrm{h})}}}. \end{aligned} \tag{13}$$

Index 1 indicates the less massive star; $R_{1,2}^{(\mathrm{h})}$ are the radii enclosing half the mass of each star. The numerical coefficients are $(c_0, c_1, \ldots c_8) = (0.525, -0.107, 6.84 \times 10^{-3}, -2.03, 0.525, 6.16 \times 10^{-4}, 0.132, 0.526, -4.89 \times 10^{-3})$.

To determine the final stellar masses, we make use of the SPH mass-loss results in the following way. First, when $M_2 > M_{\max} = 74.3\,\mathrm{M}_\odot$, we try to rescale M_1 and M_2 by some factor η bringing ηM_2 to $0.95\,M_{\max}$ while keeping $\eta M_1 > M_{\min}$. This would conserve the mass ratio q but is not possible when $q < q_{\min} = M_{\min}/M_{\max} \simeq 10^{-3}$. Such cases are relatively unimportant because, in typical cases, the VMS grows mostly by merging with 50–120 $\mathrm{M}_\odot$ stars, so $q > 0.025$ even for $M_{\mathrm{VMS}} = 2000\,\mathrm{M}_\odot$. We deal with them by rescaling M_1 to $1.05\,M_{\min}$, independently of M_2. From the SPH results, we

interpolate the fractional mass loss $\delta_M = (\delta M_1 + \delta M_2)/(M_1 + M_2)$ for the $(M_1, M_2, V_{\rm rel}^{\infty}, d_{\rm min})$ parameters of the collision (with M_1, M_2 possibly rescaled), as explained in Freitag & Benz (2005). Inspection of SPH results for fly-bys shows that only in very exceptional cases does the mass of any of the two stars increase. In fact, to a good approximation, we find the mass ratio to be conserved. We thus use this assumption to determine the individual masses from δ_M.

4 TEST SIMULATIONS

Before embarking on the large-scale numerical exploration of the runaway scenario to which Paper II is devoted, we first demonstrate that our numerical tools are up to this task. Here we check that we can reliably model the following two key aspects of the scenario: (i) fast segregation-driven core collapse in clusters with a broad mass function; and (ii) influence of collisions in cluster evolution and onset of collisional runaway.

4.1 Important quantities and units

Keeping with the tradition, when not stated otherwise, we are using the N-body unit system (Hénon 1971) defined by $G = 1$, $M_{\rm cl}(0) = 1$ (initial total cluster mass) and $U_{\rm cl}(0) = -1/2$ (initial cluster potential energy). As time-unit, we prefer the 'FP' time $T_{\rm FP}$ to the N-body unit $T_{\rm NB}$ because the former is a relaxation time while the latter is a dynamical time; they are related to each other by $T_{\rm FP} = N_*/\ln(\gamma_{\rm c} N_*)\, T_{\rm NB}$.

All test computations performed here are based on the Plummer model (Plummer 1911; Binney & Tremaine 1987) for which we recall some important quantities in Table 1.

We refer to GFR04 (section 3 and table 1) for more detailed explanations about units and the important physical parameters of a variety of clusters models.

4.2 Core collapse without collisions

4.2.1 Comparison with direct N-body simulations

In Freitag & Benz (2001), the ability of ME(SSY)**2 to follow the relaxational evolution of clusters has been successfully tested against other simulation methods for clusters with single-mass, two-component or continuous mass functions. However, in that paper, no comparison was done with direct N-body results and the only continuous mass spectrum considered was a relatively narrow 0.1–1.5 $M_\odot$ Salpeter IMF ($\mu \equiv M_{*,\rm max}/\langle M_*\rangle \simeq 2.2$). Given the importance of core collapse in clusters with $\mu > 100$ for the runaway scenario and the dearth of published data about this situation, we decided to carry out new comparisons between ME(SSY)**2 and direct N-body integrations of the core-collapse evolution of clusters with various IMFs.

Table 1. Important quantities for the Plummer model. All quantities are in N-body units except times which are in FP units.

Quantity	Symbol	Value
Plummer scale	$R_{\rm P}$	$3\pi/16 \simeq 0.589$
Core radius	$R_{\rm core}$	0.417
Half-mass radius	$R_{\rm h}$	0.769
Central density	$\rho_{\rm c}$	1.167
Central 1D velocity dispersion	$\sigma_{\rm v,c}$	0.532
Mass within $R_{\rm core}$	$M_{\rm core}$	0.193
Central relaxation time	$t_{\rm rc}$	0.0437
Half-mass relaxation time	$t_{\rm rh}$	0.0930

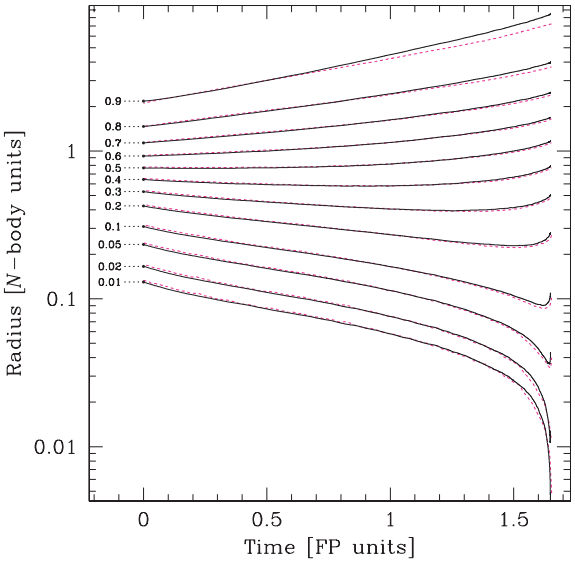

Figure 4. Core collapse of a single-mass Plummer model. We compare the results of ME(SSY)**2 with $N_{\rm p} = 300\,000$ particles (solid lines) to those of a direct N-body run with $N_{\rm p} = 65\,536$ (dotted lines, in magenta in the online colour version; from Baumgardt et al. 2003). We plot the evolution of various Lagrange radii, that is, the radii of spheres enclosing the indicated fraction of the cluster mass. For the N-body simulation, only fractions larger or equal to 1 per cent are tracked. Fractions of 3, 4, ... 9 per cent are tracked in the N-body run but not in the MC computation. A value of $\gamma_{\rm c} = 0.09$ was used in the Coulomb logarithm when converting N-body time-units into FP units to get the best agreement in core-collapse times. To improve clarity, the curves have been smoothed using a sliding average with Gaussian kernel.

The N-body simulations reported here were done with the collisional Aarseth N-body code NBODY4 (Aarseth 1999) on the GRAPE-6 boards of Tokyo University (Makino et al. 2003). Use of GRAPE-6 hardware is essential to perform N-body simulations with more than 10^5 stars within a reasonable amount of computer time. Details on the NBODY4 code can be found in Aarseth (1999), and references therein, and Baumgardt & Makino (2003).

We first checked the simplest situation, that of a single-mass cluster. In Fig. 4, we compare the evolution of the Lagrange radii of a Plummer model as obtained with NBODY4 (Baumgardt et al. 2003) and ME(SSY)**2. The agreement between the two methods is excellent if we set the coefficient in the Coulomb logarithm to $\gamma_{\rm c} = 0.09$ when converting the N-body time-units, natural to NBODY4, to FP units. Given the run-to-run variations of MC results (for different random sequences), this value is compatible with the one found by Giersz & Heggie (1994) in comparisons between N-body runs with various particle numbers ($N_{\rm p} = 250$–2000) and later confirmed by Baumgardt (2001) ($N_{\rm p} = 128$–$16\,384$), $\gamma_{\rm c} = 0.11$; it is also compatible with the one chosen by Drukier et al. (1999) to adjust their FP results to N-body simulations, $\gamma_{\rm c} = 0.10$.

After this test-run, we considered a cluster consisting of stars with masses from 0.1 to 10 $M_\odot$. The masses are distributed according to the IMF advocated by Kroupa (2001). For our simulations, the 'Kroupa IMF' corresponds to a piecewise power law: $dN_*/dM_* \propto M_*^{-\alpha}$ with $\alpha = 1.3$ below 0.5 $M_\odot$ and $\alpha = 2.3$ for higher masses. This produces a mass ratio $\mu \simeq 19.3$. Fig. 5 depicts the Lagrange radii evolution for ME(SSY)**2 and NBODY4 simulations of this model. Converting time-units with $\gamma_{\rm c} = 0.015$, we observe

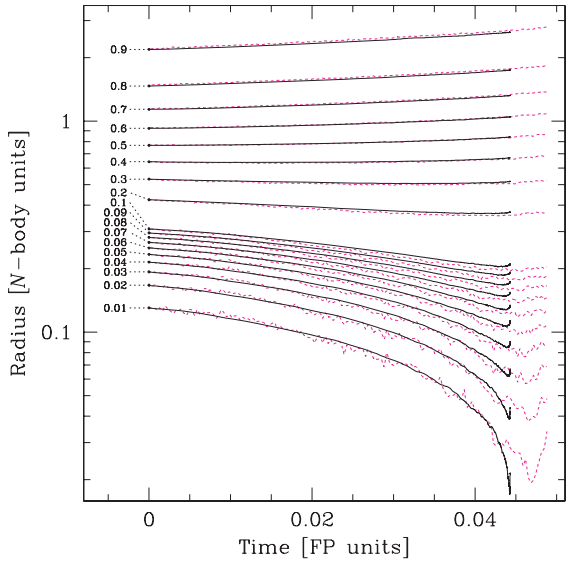

Figure 5. Evolution of Lagrange radii during the core collapse of a Plummer model with a mass spectrum. The cluster has a Kroupa mass function (see text) extending from 0.1 to 10 $M_\odot$. We compare the results of ME(SSY)**2 with $N_p = 10^6$ particles (solid lines) to those of a direct N-body run with N_p = 131 072 (dotted lines, in magenta in the online colour version). A value of $\gamma_c = 0.015$ was used in the Coulomb logarithm when converting N-body time-units into FP units to get the best overall agreement.

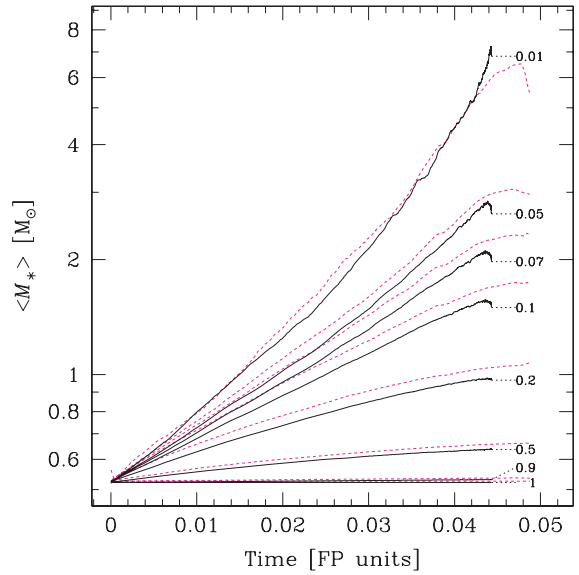

Figure 6. Mass segregation during the core collapse of a Plummer model with a mass spectrum. The data are for the same MC and N-body simulations as in Fig. 5. We plot the stellar mass averaged over all particles inside spheres containing the indicated fraction of the total mass of the cluster.

an excellent agreement between the results of both the codes until, at $t \simeq 0.043\,T_{FP}$, shortly before the moment of deepest collapse in the N-body run, it starts showing slower contraction of the innermost regions. This departure from the MC results is probably due to small-number effects, such as large-angle scatterings or binary formation, that naturally kick in the shrinking core of the N-body system (computed with N_p = 131 072) but are, by nature of the MC approach, absent from the ME(SSY)**2 run. Eventually, at $t \simeq 0.047\,T_{FP}$, three-body binaries reverse core collapse in the N-body simulation. Hénon (1975) explained why a smaller γ_c value is appropriate for systems with a mass spectrum and, from multi-mass N-body simulations with $N_p = 250$–1000, Giersz & Heggie (1996) indeed found $\gamma_c \simeq 0.015$–0.025.

In such multi-mass clusters, core collapse is driven by mass segregation. Fig. 6 allows us to witness this process by plotting the evolution of the average mass within spheres containing various fractions of the total cluster mass. Again the MC results match those of the N-body run closely.

We now consider a mass spectrum of realistic breadth, that is, a Kroupa IMF extending from 0.1 to 100 $M_\odot$, yielding $\mu \simeq 157$. To reduce numerical noise without increasing N_p to an impractically high value, we realized two N-body simulations of this system with $N_p = 131\,072$ (starting from different realizations of the initial cluster) and averaged their results. Comparisons of the Lagrange radii and average stellar mass evolutions are shown in Figs 7 and 8. This time, we stuck to $\gamma_c = 0.01$, the value we traditionally use to convert from FP time to physical time in our MC simulations of multi-mass clusters. This value turns out to yield a perfect match between the MC core-collapse time and the time of maximum contraction of the inner regions in the N-body runs. However, $\gamma_c \simeq 0.025$ would have allowed a better agreement in the early shapes of the Lagrange radii curves. At any rate, the agreement between ME(SSY)**2 and NBODY4 results is not as good as for previous cases. In particular, it appears that mass segregation is faster and stronger but more progressive

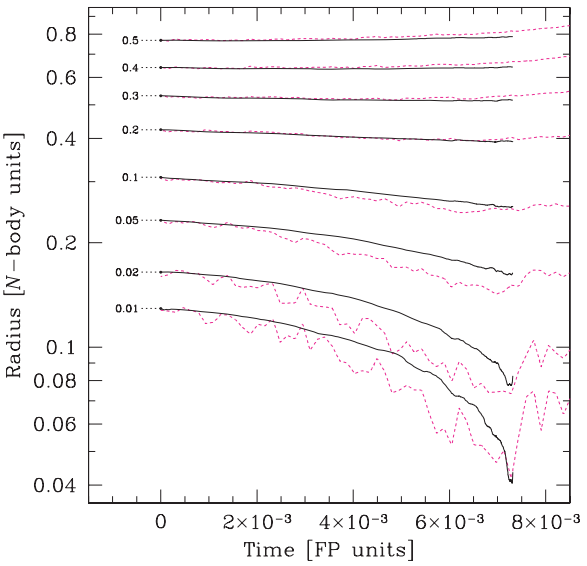

Figure 7. Evolution of Lagrange radii during the core collapse of a Plummer model with a broad mass spectrum. The cluster has a Kroupa mass function (see text) extending from 0.1 to 100 $M_\odot$. We compare the results of ME(SSY)**2 with $N_p = 1.25 \times 10^6$ particles (solid lines) to the averaged results of two direct N-body runs with $N_p = 131\,072$ (dotted lines, in magenta in the online colour version). Our standard value of $\gamma_c = 0.01$ was used in the Coulomb logarithm when converting N-body time-units into FP units.

in the N-body run. In the MC simulation, segregation accelerates at late times and the average stellar mass in the innermost regions (inside the 1 per cent Lagrange radius) reaches values similar to those found in the N-body run near the moment of collapse. A better understanding of the cause of the differences between the two simulation methods in the regime of broad IMF may be reached in future investigations thanks, in particular, to N-body simulations with higher N_p and, hence, less noise and less affected by small-

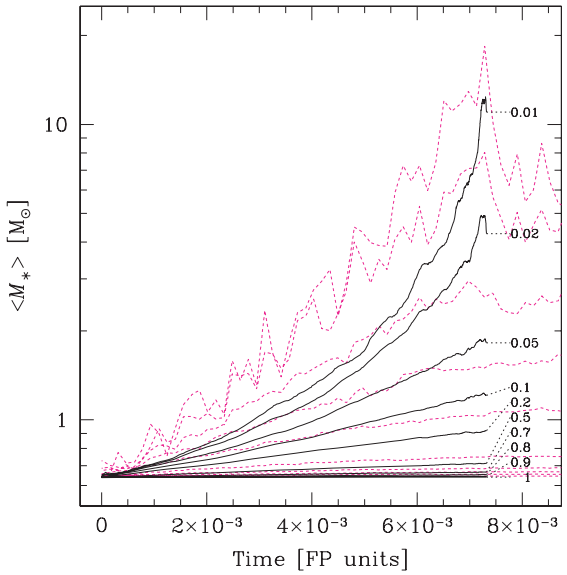

Figure 8. Mass segregation during the core collapse of a Plummer model with a broad mass spectrum. The data are for the same MC and N-body simulations as in Fig. 7. See caption of Fig. 6 for explanations about the plotted quantities.

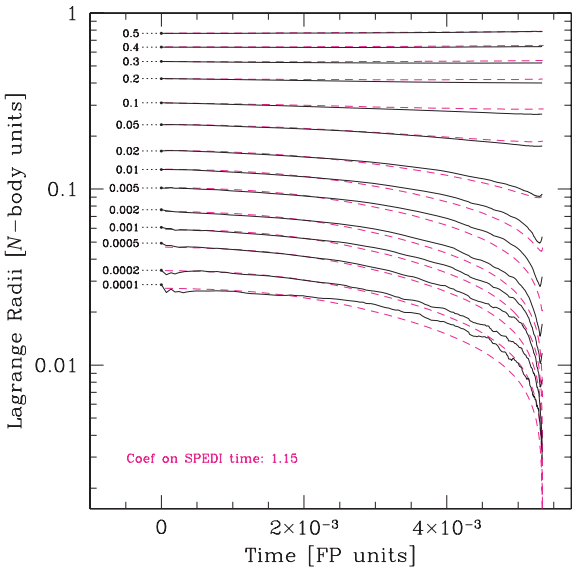

Figure 9. Evolution of Lagrange radii during the core collapse of a Plummer model with a broad mass spectrum. The cluster has a Salpeter mass function extending from 0.2 to 120 $M_\odot$. We compare the results of ME(SSY)**2 with $N_p = 1.25 \times 10^6$ particles (solid lines) to those obtained with SPEDI (with dotted lines, in magenta in the online colour version). In order to allow a better comparison of the shapes of the curves, we aligned the core-collapse times by multiplying the time-units for the SPEDI run by a factor of 1.15.

number effects in the central regions. For the moment, we note that the ME(SSY)**2 evolution of this broad-IMF cluster is qualitatively similar to that shown by the direct N-body integration and that good quantitative agreement is obtained for the aspects most important to the present investigation of the collisional runaway, namely the core-collapse time and the degree of mass segregation reached in the central regions during late collapse. The core-collapse time we obtain with ME(SSY)**2 is $t_{cc} \simeq 7.3 \times 10^{-3}\, T_{FP} = 7.9 \times 10^{-2}\, t_{rh}(0) = 0.17\, t_{rc}(0)$, in agreement with the value of $t_{cc} \simeq 0.15\, t_{rc}(0)$ found in GFR04 for systems with $\mu \gtrsim 50$.

As for the value of γ_c, we decided to stay on the conservative side by keeping it at 0.01. This is probably slightly too small, hence predicting a core-collapse evolution too *slow* with respect to other time-scales, most importantly that for stellar evolution, but the difference in relaxation time compared to, say, $\gamma_c \simeq 0.025$ is smaller than 10 per cent for $N_* \geqslant 10^6$.

4.2.2 *Comparison with the gaseous model*

The direct N-body method represents the most accurate but most computationally expensive way of simulating the secular evolution of a stellar cluster, subject to relaxation. Unfortunately, precisely because it treats gravitation in such a direct fashion, it offers no or little clean and easy way of establishing the global behaviour that a system may exhibit in the limit of very large number of stars ($N_* \gg 10^5$) from the results of simulations made with much fewer particles and ridden with noise and small-N effects.

A nearly opposite approach is taken in SPEDI, a cluster evolution code developed by R. Spurzem and collaborators (Louis & Spurzem 1991; Giersz & Spurzem 1994; Spurzem & Takahashi 1995; Amaro-Seoane, Freitag & Spurzem 2004).[7] Here, like in the MC scheme, the star system is treated in a explicitly statistical manner which assumes a very large number of stars. By taking velocity moments of the Boltzmann equation up to the second order, one obtains a set of partial differential equations for the evolution of density, average (radial) velocity and velocity dispersions (radial and tangential) of the stars at each position in the (spherical) cluster. These equations are similar to those governing the structure of self-gravitating spherical gas cloud. The effects of two-body relaxation are treated through local prescriptions for heat conduction among stars of the same mass and energy exchange between stars of different masses. This method, although approximative, allows fast simulations and smooth results because the cluster is treated as a continuum. In this scheme, the mass spectrum has to be discretized into a number of components, each representing stars of a given mass.

In Fig. 9, we compare the evolution of Lagrange radii, as obtained with ME(SSY)**2 and SPEDI, for a cluster with a Salpeter IMF ($dN_*/dM_* \propto M_*^{-2.35}$) extending from 0.2 to 120 $M_\odot$. The SPEDI simulation is the same as presented in fig. 2 of GFR04; it was carried out using $N_{comp} = 50$ mass components. Our tests show that the results depend very little on N_{comp} as soon as more than ~12 components are used. We have set the gaseous model parameters to their standard values: the coefficient in the thermal conductivity relation is $\lambda = 0.4977$ (Giersz & Spurzem 1994) and equipartition time is set by $\lambda_{eq} = 1$ (Spurzem & Takahashi 1995). We note that SPEDI produces a collapse some 13 per cent faster than ME(SSY)**2, a difference that may be the result of a slightly inadequate value of λ_{eq} as this parameter has been determined only for the case of two-component models, by comparison with N-body and FP simulations (Spurzem & Takahashi 1995). In the figure, we have rescaled the time of the gaseous-model simulation to obtain the same t_{cc} as in the MC run. The evolution to core collapse is just slightly more progressive in the SPEDI run but the agreement is otherwise very good, given the important differences in both numerical approaches. The core-collapse time we obtain is $t_{cc} \simeq 5.4 \times 10^{-3}\, T_{FP} = 5.8 \times 10^{-2}\, t_{rh}(0) = 0.12\, t_{rc}(0)$, ~20 per cent faster than in GFR04. This

[7] SPEDI is maintained at the Astronomisches Rechen-Institut in Heidelberg, see http://www.ari.uni-heidelberg.de/gaseous-model.

difference reflects not only differences between the two MC codes but also intrinsic variations in t_{cc} obtained between ME(SSY)**2 runs computed for the same initial conditions but with different random sequences (see fig. 2 of Paper II).

4.3 Runaway collisions: comparison with Quinlan & Shapiro (1990)

In Freitag & Benz (2002b), we have already checked that ME(SSY)**2 produces the correct rate of collisions, both as a function of the distance to the centre of the cluster and of the masses of stars, for multi-mass clusters. We have also reproduced the overall results of collisional models of MBH-hosting galactic nuclei considered by Duncan & Shapiro (1983) and Murphy et al. (1991). In such environments, however, collisions occur at very high relative velocities and do not lead to runaway growth (Freitag et al. 2004).

To our knowledge, QS90, using an FP code, were the first to study in a systematic way the process of collisional runaway accounting self-consistently for cluster dynamics and secular evolution and how collisions themselves affect it.

We have run simulations for all six 'E' models of QS90, assuming, in most cases, sticky-sphere collisions and complete rejuvenation for each merger as these authors did. Initial conditions are high-density Plummer clusters with all stars of solar type, with various total masses and sizes. Table 2 lists the characteristics of these models. Stellar evolution is included. QS90 implemented it in a simplified way, similar to ours. However, while we can assign an individual age to each MC particle (which represents 4.2 to 36 stars, depending on the model), in the FP scheme of QS90 only a small number of discrete mass components are present (for stars of mass $2^i\,M_\odot$ with $i = 1, 2, \ldots 8$), each of which represents some homogeneous population. Stellar evolution can only be treated in statistical way, with each component having an average age. Similarly, collisions can only be accounted for statistically by integrating merger rates within and between mass components and distributing the number of merger products over components in a way that conserve total mass but not necessarily individual stellar masses because not all possible merger masses are represented. Unlike QS90, we have allowed for collisions between MS stars and compact remnants by assuming complete disruption of the MS star but no change to the mass or velocity of the compact object. Certainly an oversimplification, this prescription obviously corresponds to the most unfavourable possible one, as far as collisional runaway is concerned. To have the same ratios between the time-scale for relaxation and that for other processes (collisions, stellar evolution) as QS90, we adopt their $\gamma_c = 0.4$ value for this set of simulations.

In contrast to QS90, we find core collapse and collisional runaways in all cases but E2B whose core contraction is stopped by the mass loss due to stellar evolution of collision products.

Agreement for model E4A is very satisfying: in our model QS90-E4A, we find core collapse and runaway to happen at $t_{cc} \simeq 140$ Myr $\simeq 1.44\,t_{rh}(0)$, to compare with QS90's value of ∼130 Myr. Without collisions, a single-mass Plummer model would experience core collapse at $t_{cc} \simeq 17$–$18\,t_{rh}(0)$, so mergers clearly play an important role in the cluster evolution from the beginning, by dissipating energy and creating a mass spectrum, hence allowing mass segregation. For this reason, one cannot predict the occurrence of runaway in those clusters just from the relaxational value of the core-collapse time, $t_{cc}|_{rlx}$. Also, even though all stars are initially of $1\,M_\odot$, it is not sufficient to have $t_{cc}|_{rlx} < 10$ Gyr for collisional runaway to kick in. Paradoxically, if merger products are formed before deep collapse they may be able to stop collapse as they evolve off the MS much earlier, as happens in our case E2B (QS90-E2B).

Fig. 10 shows the evolution of the Lagrange radii our simulation of case E4A. We have also redone the simulation with the more realistic prescriptions for collision outcomes based on SPH simulations (QS90-E4Asph). As can be seen in Fig. 10, when collisional mass loss and, more importantly, fly-by, non-merging collisions are accounted for, the cluster evolution is significantly slower. This is because, in clusters with such a high-velocity dispersion [$\sigma_{v,c}(0) \simeq 231\,\mathrm{km\,s^{-1}}$], only a minority of collisions result in mergers, amounting to a reduction in the effective collision cross-sections. In Fig. 11, we have plotted the evolution of the number of stars of various masses during the evolution of QS90-E4A. The evolution of the number of stars of mass 2–3 $M_\odot$ in our run is nearly identical to that of the 2-$M_\odot$ component of QS90 but we obtain significantly fewer stars more massive than $3\,M_\odot$. This demonstrates that the rate of collision between $1\,M_\odot$ (and hence, of formation of first-generation mergers) is the same in both simulations. Because QS90's FP method imposes a completely different (and much less physical) way of dealing with mergers of mergers, it is not surprising no close agreement is reached on that matter. The *M–R* relation cannot be blamed, however, as they assume $R_*/R_\odot = (M_*/M_\odot)^{0.55}$, which is close to our relation. The drop in the number of stars more massive than $16\,M_\odot$ at the end of our simulation corresponds to

Table 2. Cluster simulations for comparison with QS90.

Name	Name in QS90	N_*	N_p	R_{NB} (pc)	t_{cc} (T_{FP})	t_{cc} (Myr)
QS90-E4A	E4A	1.8×10^7	5×10^5	0.41	0.134	141
QS90-E4Ahr	E4A	1.8×10^7	2.1×10^6	0.41	0.129	136
QS90-E4Asph[a]	E4A	1.8×10^7	5×10^5	0.41	0.275	289
QS90-E4B	E4B	3.1×10^7	5×10^5	0.71	0.182	553
QS90-E4Bb[b]	E4B	3.1×10^7	5×10^5	0.71	0.172	522
QS90-E4Ac[c]	E4B	3.1×10^7	5×10^5	0.71	0.189	574
QS90-E2A	E2A	6.2×10^6	5×10^5	0.565	0.371	397
QS90-E2B	E2B	1.1×10^7	5×10^5	1.00	[d]	...
QS90-E1A	E1A	2.1×10^6	5×10^5	0.765	0.758	803
QS90-E1B	E1B	3.6×10^6	5×10^5	1.31	1.23	3680
QS90-E4Ab[e]	E1B	3.6×10^6	5×10^5	1.31	1.24	3710

[a]Collision prescriptions based on SPH data. Minimal rejuvenation. [b]Other random sequence than for QS90-E4B. [c]Time-step four times larger than for QS90-E4B. [d]Core collapse stopped by stellar evolution. [e]Other random sequence than for QS90-E1B.

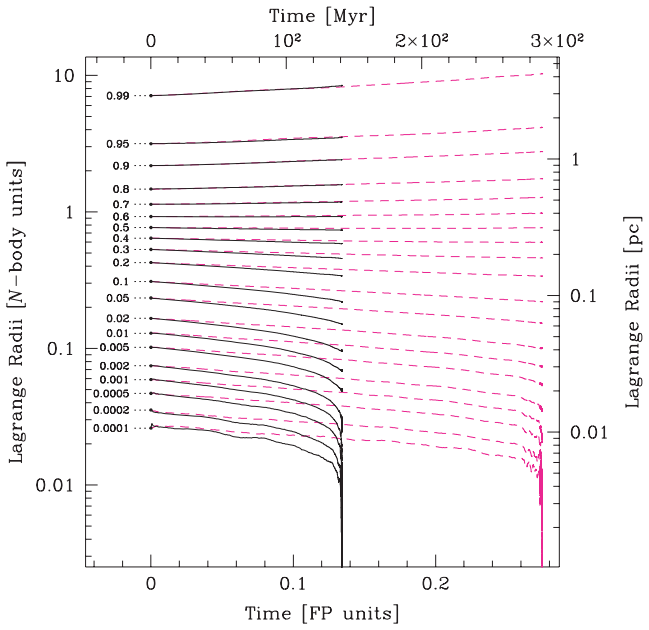

Figure 10. Evolution of Lagrange radii in core collapse with stellar collisions. The initial conditions are those of model E4A of QS90. We present two simulations. In the first one (solid lines, QS90-E4A), all collisions are treated as pure mergers with complete rejuvenation. In the second case (dashed lines, QS90-E4Asph), we use SPH-inspired collision prescriptions and minimal rejuvenation.

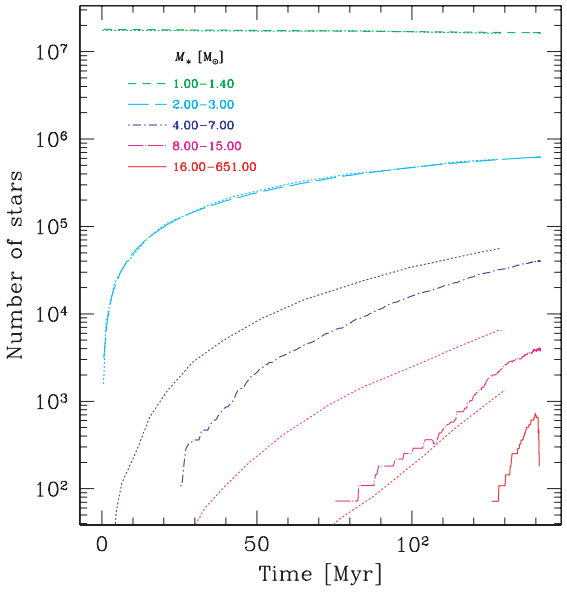

Figure 11. Number of stars in various mass bins during cluster evolution with stellar collisions. Same simulation as in Fig. 10 (QS90-E4A). Dotted lines are the results of QS90 (their fig. 2a) for mass components of mass 1, 2, 4, 8 and $\geqslant 16\,M_\odot$. The curves for 1 and $2\,M_\odot$ are nearly indistinguishable from ours (for 1–1.4 and 2–3 $M_\odot$ bins). We obtain a lower number of stars more massive than $3\,M_\odot$ than QS90. At the end of our simulation, ∼200 white dwarfs and a similar number of neutron stars have formed. The (negligible) contribution of neutron stars is included in the first mass bin; white dwarfs are not plotted. We used 5×10^5 particles for our simulation so each of them represents 36 stars.

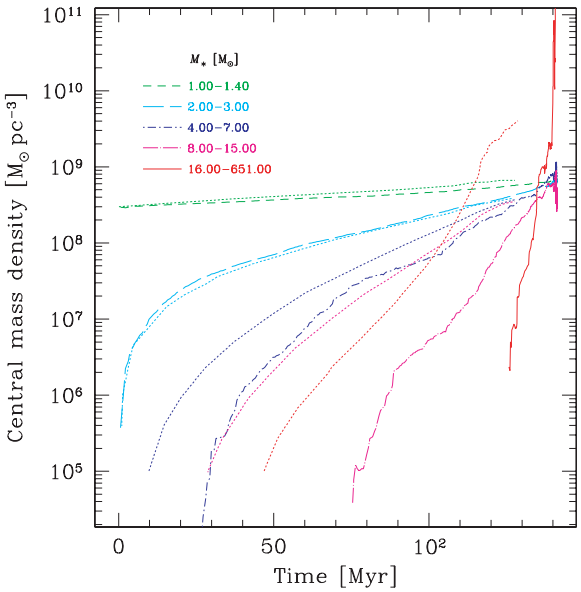

Figure 12. Mass density of stars of various masses in the central region of a cluster during its evolution with stellar collisions. Same simulation as in Figs 10 and 11 (QS90-E4A). For the 1–1.4, 2–3, 4–7, 8–15 and $\leqslant 16\,M_\odot$ mass bin, we plot the average density within a sphere containing, respectively, a fraction 0.001, 0.01, 0.01, 0.1 and 0.1 of the total mass in the corresponding range of stellar masses. As in Fig. 11, thin dotted lines indicate results of QS90 (their fig. 2b). Note that the curve from QS90 closest to our line for the 4–7 $M_\odot$ bin is for their 8-$M_\odot$ mass component.

the runaway growth of a VMS by merging between massive stars. When we stopped our run, the VMS had reached 651 $M_\odot$. We refer to Paper II for a discussion of physical processes that may terminate the VMS growth, most of which are lacking from ME(SSY)**2. How mergers create a population of massive stars which come to dominate the central region of the cluster is further indicated by Fig. 12. Here, we follow the contribution to the central density of stars in various mass ranges. Unlike QS90, we cannot determine the density at $R = 0$ but have to sum the mass in some small spherical volume to estimate it. Our values are therefore lower limits. Still, the agreement for the lowest two mass bins (1–1.4 $M_\odot$ and 2–3 $M_\odot$) is very satisfying, but again, we get considerably fewer higher-mass stars.

Although three times less massive, model E4B has the same velocity dispersion as E4A and, hence a very similar initial value of $t_{\rm rlx}/t_{\rm coll}$ (up to small differences in Coulomb logarithms). Therefore, one could have expected collisions to play the same role and to get the same value of $t_{\rm cc}/t_{\rm rh}(0)$. However, stellar evolution introduce still another time-scale in the problem and because $t_{\rm rh}(0)$ is longer (in years) for model E4A, more collision products have time to evolve off the MS, which delays core collapse. At $t = 0.13\,T_{\rm FP}$, the fractional number of white dwarfs in our E4A run is $\sim 10^{-5}$ while it reaches $\sim 10^{-3}$ in run E4B. In QS90's run for this case, stellar evolution was able to stop core collapse around $t \approx 700$ Myr, before any star more massive than $32\,M_\odot$ formed. In contrast, our models produced a runaway merger after 520–570 Myr already. The evolution of number of stars of different masses is plotted in Fig. 13 and compared with QS90's results (for the contraction phase). Again, the agreement with QS90 is excellent for the 2–3 $M_\odot$ mass bin but poorer for others. This time, our run produces more massive stars (after $t \approx 300$ Myr), which eventually leads to runaway. Clearly, because the evolution is driven by a positive feedback loop

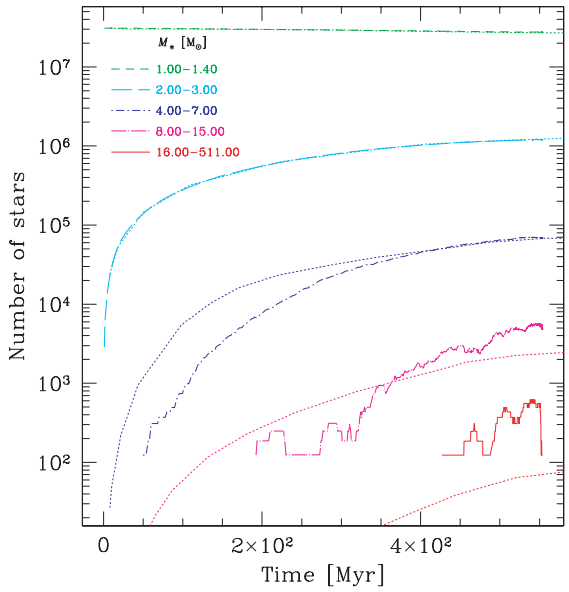

Figure 13. Number of stars in various mass bins during cluster evolution with stellar collisions. Our simulation for model E4B (QS90-E4B) is compared to data from QS90 (their fig. 4a). See caption of Fig. 11 for explanations.

between mass segregation and collisions and because only stellar evolution of merger products themselves can revert it, differences in the treatment of collisions may have very important effects.

For their other 'E' models, QS90 only indicate the end state in a very succinct way, giving no details about the evolution. For model E2A, we find runaway at $t \simeq 400$ Myr, to be compared with QS90's value of $t \simeq 490$ Myr, a satisfying agreement, given how different the approaches are. Model E2B is prevented from entering the runaway phase by stellar evolution in both QS90's and our simulation. In our simulation (QS90-E2B), a few particles grow to 8 $M_\odot$ and one to 11 $M_\odot$ during the phase of central concentration. QS90 report that the most massive stars formed have 8 $M_\odot$ in this case. In QS90, the core collapse of model E1A is reversed by the formation of, and energy input from three-body binaries, a process we do no take into consideration (see discussion in Appendix A), but the fact that they form stars as massive as 64 $M_\odot$ indicates that they nearly reach the conditions for runaway. For this cluster we obtain runaway at $t \simeq 800$ Myr. Finally, E1B is another case for which QS90 find the core collapse is interrupted by stellar evolution but our simulation produces runaway at $t \simeq 0.37$ Gyr. In one of our simulations for this model, the runaway star is destroyed in a collision with a compact object, just after it has reached a mass of 157 $M_\odot$. Another runaway sequence starts shortly afterwards.

Since QS90, runaway collisions in clusters have been studied by use of the direct N-body method (Portegies Zwart et al. 1999a; Portegies Zwart & McMillan 2002; Portegies Zwart et al. 2004). Unfortunately, these simulations were either limited to $N_p \lesssim 10^5$, in which case binaries play a crucial role or, for the few cases reaching $N_p \simeq 6 \times 10^5$ and experiencing runaway, done for clusters with high initial concentration (King parameter $W_0 \geqslant 9$) and, hence probably dominated by small-number effects in the innermost regions. In Paper II, we report briefly on the simulations we have done with initial conditions similar to those of some models of Portegies Zwart et al. (2004).

5 SUMMARY

The results presented here are mostly tests to ensure that the MC stellar dynamics code we use, ME(SSY)**2 (Freitag & Benz 2001, 2002b), correctly treats the following key processes at play in the runaway route.

(i) Mass segregation-induced core collapse, driven by two-body relaxation in cluster with a broad, realistic mass function (Salpeter of Kroupa, with $M_{*,\min} = 0.1$–$0.2\,M_\odot$ and $M_{*,\max} \simeq 100\,M_\odot$)
(ii) Effects of collisions in the evolution of the cluster and occurrence of collisional runaway.

This paper is a companion to Paper II in which we present the results of our large set of simulations to determine the conditions for, and characteristics of collisional runaway in young stellar clusters. In the scenario we investigate, the collisional phase is brought up by the concentration, through relaxation, of massive stars in the centre of a cluster. A star much more massive than 100 $M_\odot$, formed in a quick sequence of collisions may not only be a progenitor for an IMBH but is in itself an exotic object of considerable interest.

To address point (i), we performed simulations of clusters with ME(SSY)**2, NBODY4 and the gaseous-model code SPEDI. The only physical process included in the MC and gaseous-model runs was two-body relaxation, treated in the standard FP approximation, that is, as the sum of uncorrelated small-angle two-body scatterings whose rate is determined by local conditions at each point in the cluster. The N-body code treats Newtonian gravitation in an essential exact way, without assumptions about the nature of relaxation. ME(SSY)**2 produces results in close agreement with their N-body counterparts for $\mu = M_{*,\max}/\langle M_* \rangle \leqslant 20$ at least. Realistic IMF corresponds to $\mu \gtrsim 100$, however. There are clear discrepancies between the MC and N-body simulations in this regime. Most notably N-body results show an initially stronger but more progressive concentration of massive stars in the central regions. Nevertheless, the most important characteristics of the core collapse as a path to the collisional runaway stage, namely the time for it to happen, t_{cc}, and the magnitude of central mass segregation during deep collapse are similar in both type of simulations. Furthermore, SPEDI yields results very close to those of ME(SSY)**2, except for a value of t_{cc} 13 per cent shorter.

Turning now to point (ii), we note that only very few numerical simulations of the evolution of clusters subject to relaxation and collisions, up to and including the runaway stage have been published. Putting aside the recent N-body runaway simulations (Portegies Zwart et al. 1999a; Portegies Zwart & McMillan 2002; Portegies Zwart et al. 2004), not suitable for clear-cut comparison with ME(SSY)**2 results as small-N effects may play a strong role in them, we are left with the older FP simulations of QS90. These models lack realism because they start with a single-mass population of 1-$M_\odot$ stars. Collisions are assumed to result in perfect mergers, with no mass loss. In most cases considered, the cluster is dense enough to promote stellar mergers at early times. The more massive stars thus formed accelerate collapse by mass segregation, hence further increasing the merger rate. These same merger products can also terminate the process of central density build-up through their mass loss when they evolve off the MS, well before the original 1 $M_\odot$ would have done so.

We have simulated the six models of QS90 for which these authors have assumed that the gas lost through stellar evolution escapes the cluster (rather than staying in it and forming new stars). Although collisional runaway happens more often in our simulations than in QS90 runs, we obtain good general agreement with the relatively

scarce data published by QS90. For the two situations in which they report core collapse uninterrupted by stellar evolution or three-body binaries, we obtain core-collapse times 8 per cent longer and 18 per cent shorter than theirs, which we find satisfying considering the widely different numerical methods and, especially, treatments of collisions, of critical importance here. The production rate of 2–3 $M_\odot$ objects in our runs is nearly exactly the same as for QS90's 2-$M_\odot$ mass bin but notable differences exist for higher-mass objects, which, resulting from longer merger sequences, are more affected by differences in treatments of collisions. For a large part, the discrepancies between ours and QS90's certainly originates in this. Our treatment of collisions being much more direct and accurate than the one allowed by the FP code of QS90, the differences found in these comparisons do not cast doubt on the ability of ME(SSY)**2 to deal with collisional cluster evolution.

We have also re-simulated one of the QS90 models with the highest velocity dispersion using our more realistic treatment of collisions, based on SPH simulations (Freitag & Benz 2005) and found a significantly longer core-collapse time due to the collisions being less effective at producing higher-mass stars. This stresses the importance of using collision prescriptions which account for flybys and mass loss, in the high-velocity regime. This question is investigated in more depth in Paper II.

ACKNOWLEDGMENTS

We thank Melvyn Davies, John Fregeau, M. Atakan Gürkan, Jamie Lombardi, Simon Portegies Zwart, Rainer Spurzem and Hans Zinnecker for useful discussions. We are grateful to Rainer Spurzem for making the code for gaseous models (SPEDI) available and for his assistance in using it. MF is indebted to Pau Amaro Seoane for his extraordinary support during his stay in Heidelberg. The work of MF was funded in part by the Sonderforschungsbereich (SFB) 439 'Galaxies in the Young Universe' (subproject A5) of the German Science Foundation (DFG) at the University of Heidelberg. This work was also supported by NASA ATP Grants NAG5-13236 and NNG04G176G, and NSF Grant AST-0206276 to Northwestern University.

REFERENCES

Aarseth S. J., 1999, PASP, 111, 1333
Amaro-Seoane P., Freitag M., Spurzem R., 2004, MNRAS, 352, 655
Bally J., Zinnecker H., 2005, AJ, 129, 2281
Baraffe I., Heger A., Woosley S. E., 2001, ApJ, 550, 890
Baumgardt H., 2001, MNRAS, 325, 1323
Baumgardt H., Heggie D. C., Hut P., Makino J., 2003, MNRAS, 341, 247
Baumgardt H., Makino J., 2003, MNRAS, 340, 227
Baumgardt H., Makino J., Ebisuzaki T., 2004a, ApJ, 613, 1133
Baumgardt H., Makino J., Ebisuzaki T., 2004b, ApJ, 613, 1143
Begelman M. C., Rees M. J., 1978, MNRAS, 185, 847
Belczynski K., Kalogera V., Bulik T., 2002, ApJ, 572, 407
Benz W., 1990, in Buchler J. R., ed., Numerical Modelling of Nonlinear Stellar Pulsations Problems and Prospects. p. 269
Benz W., Hills J. G., 1987, ApJ, 323, 614
Benz W., Hills J. G., 1992, ApJ, 389, 546
Binney J., Tremaine S., 1987, Galactic Dynamics. Princeton Univ. Press, Princeton, NJ
Blandford R. D., 2004, in Ho L., ed., Coevolution of Black Holes and Galaxies, from the Carnegie Observatories Centennial Symposia. Cambridge Univ. Press, Cambridge, p. 154
Bond J. R., Arnett W. D., Carr B. J., 1984, ApJ, 280, 825
Bonnell I. A., Bate M. R., Zinnecker H., 1998, MNRAS, 298, 93
Campbell B. et al., 1992, AJ, 104, 1721
Chabrier G., Baraffe I., 2000, ARA&A, 38, 337
Chandrasekhar S., 1960, Principles of Stellar Dynamics. Dover Press, New York
Charbonnel C., Däppen W., Schaerer D., Bernasconi P. A., Maeder A., Meynet G., Mowlavi N., 1999, A&AS, 135, 405
Chernoff D. F., Huang X., 1996, in Hut P., Makino J., eds, IAU Symp. 174, Dynamical Evolution of Star Clusters: Confrontation of Theory and Observations. p. 263
Colgate S. A., 1967, ApJ, 150, 163
Collins N. A., Hughes S. A., 2004, Phys. Rev. D, 69, 124022
Cutler C., Thorne K. S., 2002, in Bishop N., Mahara S. D., eds, Proc. GR 16. World Scientific, Singapore, p. 72
Dehnen W., 1993, MNRAS, 265, 250
Drukier G. A., Cohn H. N., Lugger P. M., Yong H., 1999, ApJ, 518, 233
Duncan M. J., Shapiro S. L., 1983, ApJ, 268, 565
Ebisuzaki T. et al., 2001, ApJ, 562, L19
Fabian A. C., Iwasawa K., 1999, MNRAS, 303, L34
Fabian A. C., Pringle J. E., Rees M. J., 1975, MNRAS, 172, 15
Figer D. F., 2004, in Lamers H. J. G. L. M., Smith L. J., Nota A., eds, ASP Conf. Ser. Vol. 322, The Formation and Evolution of Massive Young Star Clusters. Astron. Soc. Pac., San Francisco, p. 49
Figer D. F., Najarro F., Morris M., McLean I. S., Geballe T. R., Ghez A. M., Langer N., 1998, ApJ, 506, 384
Figer D. F., McLean I. S., Morris, 1999, ApJ, 514, 202
Fregeau J. M., Cheung P., Portegies Zwart S. F., Rasio F. A., 2004, MNRAS, 352, 1
Freitag M., 2000, PhD thesis, Université de Genève
Freitag M., 2001, Classical and Quantum Gravity, 18, 4033
Freitag M., Benz W., 2001, A&A, 375, 711
Freitag M., Benz W., 2002a, in Shara M., ed., ASP Conf. Ser. Vol. 263, Stellar collisions & mergers and their consequences. Astron. Soc. Pac., San Francisco, p. 261
Freitag M., Benz W., 2002b, A&A, 394, 345
Freitag M., Benz W., 2005, MNRAS, 358, 1133
Freitag M., Gürkan M. A., Rasio F. A., 2004, in St-Louis N., Moffat A., eds, Massive Stars in Interacting Binaries. Preprint (astro-ph/0410327)
Freitag M., Gürkan M. A., Rasio F. A., 2005, MNRAS, this issue (doi:10.1111/j.1365-2966.2006.10096.x) Paper II)
Fryer C. L., Kalogera V., 2001, ApJ, 554, 548
Gallagher J. S., Smith L. J., 1999, MNRAS, 304, 540
Gebhardt K., Rich R. M., Ho L. C., 2002, ApJ, 578, L41
Geha M., Guhathakurta P., van der Marel R. P., 2002, AJ, 124, 3073
Gerssen J., van der Marel R. P., Gebhardt K., Guhathakurta P., Peterson R. C., Pryor C., 2002, AJ, 124, 3270
Giersz M., Heggie D. C., 1994, MNRAS, 268, 257
Giersz M., Spurzem R., 1994, MNRAS, 269, 241
Giersz M., Heggie D. C., 1996, MNRAS, 279, 1037
Giersz M., Spurzem R., 2003, MNRAS, 343, 781
Goodman J., Hernquist L., 1991, ApJ, 378, 637
Goodman J., Hut P., 1993, ApJ, 403, 271
Gürkan M. A., Rasio F. A., 2005, ApJ, 628, 236
Gürkan M. A., Freitag M., Rasio F. A., 2004, ApJ, 604, 632 (GFR04)
Gürkan M. A., Fregeau J. M., Rasio F. A., 2006, ApJ, in press (astro-ph/0512642)
Haehnelt M. G., Kauffmann G., 2002, MNRAS, 336, L61
Haehnelt M. G., Natarajan P., Rees M. J., 1998, MNRAS, 300, 817
Hansen B. M. S., Milosavljević M., 2003, ApJ, 593, L77
Häring N., Rix H.-W., 2004, ApJ, 604, L89
Harris W. E., 1996, AJ, 112, 1487
Heger A., Fryer C. L., Woosley S. E., Langer N., Hartmann D. H., 2003, ApJ, 591, 288
Heggie D., Hut P., 2003, The Gravitational Million-Body Problem: A Multidisciplinary Approach to Star Cluster Dynamics. Cambridge Univ. Press, Cambridge
Hénon M., 1971, Ap&SS, 13, 284
Hénon M., 1973, in Martinet L., Mayor M., eds, Dynamical structure and evolution of stellar systems, Lectures of the 3rd Advanced Course of the Swiss Society for Astronomy and Astrophysics (SSAA). p. 183

Hénon M., 1975, in Hayli A., ed., IAU Symp. 69, Dynamics of Stellar Systems. p. 133
Ho L. C., Filippenko A. V., 1996, ApJ, 472, 600
Hughes S. A., Holz D. E., 2003, Classical and Quantum Gravity, 20, 65
Hurley J. R., Pols O. R., Tout C. A., 2000, MNRAS, 315, 543
Ishii M., Ueno M., Kato M., 1999, PASJ, 51, 417
Ivanova N., Belczynski K., Fregeau J. M., Rasio F. A., 2005, MNRAS, 358, 572
Kim S. S., Lee H. M., 1999, A&A, 347, 123
Kim S. S., Figer D. F., Morris M., 2004, ApJ, 607, L123
Kroupa P., 2001, MNRAS, 322, 231
Kroupa P., Tout C. A., Gilmore G., 1993, MNRAS, 262, 545
Kudritzki R. P., 2002, ApJ, 577, 389
Kumar P., Goodman J., 1996, ApJ, 466, 946
Lai D., Rasio F. A., Shapiro S. L., 1993, ApJ, 412, 593
Lee H. M., 1987, ApJ, 319, 801
Lee M. H., 1993, ApJ, 418, 147
Lee M. H., 2000, Icarus, 143, 74
Lejeune T., Schaerer D., 2001, A&A, 366, 538
Lightman A. P., Shapiro S. L., 1978, Rev. Mod. Phys., 50, 437
Lombardi J. C. J., Rasio F. A., Shapiro S. L., 1995, ApJ, 445, L117
Lombardi J. C., Warren J. S., Rasio F. A., Sills A., Warren A. R., 2002, ApJ, 568, 939
Louis P. D., Spurzem R., 1991, MNRAS, 251, 408
Mackey A. D., Gilmore G. F., 2003, MNRAS, 338, 85
Magorrian J. et al., 1998, AJ, 115, 2285
Maillard J. P., Paumard T., Stolovy S. R., Rigaut F., 2004, A&A, 423, 155
Makino J., Fukushige T., Koga M., Namura K., 2003, PASJ, 55, 1163
Malyshkin L., Goodman J., 2001, Icarus, 150, 314
McCrady N., Gilbert A. M., Graham J. R., 2003, ApJ, 596, 240
McMillan S. L. W., 1986, ApJ, 306, 552
McMillan S. L. W., McDermott P. N., Taam R. E., 1987, ApJ, 318, 261
Menou K., 2003, Classical and Quantum Gravity, 20, 37
Merritt D., Ferrarese L., 2001, ApJ, 547, 140
Miller M. C., 2005, ApJ, 618, 426
Miller G. E., Scalo J. M., 1979, ApJS, 41, 513
Moffat A. F. J., Drissen L., Shara M. M., 1994, ApJ, 436, 183
Monaghan J. J., 1992, ARA&A, 30, 543
Murphy B. W., Cohn H. N., Durisen R. H., 1991, ApJ, 370, 60
Palla F., 2002, in Maeder A., Meynet G., eds, Physics of Star Formation in Galaxies, Lectures of the 29th Advanced Course of the Swiss Society for Astronomy and Astrophysics (SSAA). p. 9
Phinney E. S., 2003, AAS/High Energy Astrophysics Division, 7, #27.03
Plummer H. C., 1911, MNRAS, 71, 460
Podsiadlowski P., 1996, MNRAS, 279, 1104
Portegies Zwart S. F., Meinen A. T., 1993, A&A, 280, 174
Portegies Zwart S. F., McMillan S. L. W., 2002, ApJ, 576, 899
Portegies Zwart S. F., Makino J., McMillan S. L. W., Hut P., 1999a, A&A, 348, 117
Portegies Zwart S. F., Makino J., McMillan S. L. W., Hut P., 1999b, A&A, 348, 117
Portegies Zwart S. F., Baumgardt H., Hut P., Makino J., McMillan S. L. W., 2004, Nat, 428, 724
Quinlan G. D., Shapiro S. L., 1990, ApJ, 356, 483 (QS90)
Rasio F. A., Lombardi J. C., 1999, Journal of Computational and Applied Mathematics, 109, 213
Richstone D., 2004, in Ho L., ed., Coevolution of Black Holes and Galaxies, from the Carnegie Observatories Centennial Symposia. Cambridge Univ. Press, Cambridge, p. 281
Sanders R. H., 1970, ApJ, 162, 791
Schaerer D., 2002, A&A, 382, 28
Schaller G., Schaerer D., Meynet G., Maeder A., 1992, A&AS, 96, 269
Sesana A., Haardt F., Madau P., Volonteri M., 2004, ApJ, 611, 623
Sills A., Lombardi J. C., Bailyn C. D., Demarque P., Rasio F. A., Shapiro S. L., 1997, ApJ, 487, 290
Sills A., Faber J. A., Lombardi J. C., Rasio F. A., Warren A. R., 2001, ApJ, 548, 323
Sills A., Adams T., Davies M. B., Bate M. R., 2002, MNRAS, 332, 49
Sołtan A., 1982, MNRAS, 200, 115
Spitzer L., 1987, Dynamical evolution of globular clusters. Princeton Univ. Press, Princeton, NJ
Spitzer L. J., Saslaw W. C., 1966, ApJ, 143, 400
Spurzem R., Takahashi K., 1995, MNRAS, 272, 772
Stothers R. B., Chin C., 1997, ApJ, 489, 319
Tremaine S., Richstone D. O., Byun Y., Dressler A., Faber S. M., Grillmair C., Kormendy J., Lauer T. R., 1994, AJ, 107, 634
van der Marel R. P., Gerssen J., Guhathakurta P., Peterson R. C., Gebhardt K., 2002, AJ, 124, 3255
Vink J. S., de Koter A., Lamers H. J. G. L. M., 2001, A&A, 369, 574
Volonteri M., Haardt F., Madau P., 2003, ApJ, 582, 559
Walcher C. J. et al., 2005, ApJ, 618, 237
Wyithe J. S. B., Loeb A., 2003, ApJ, 595, 614
Yu Q., Tremaine S., 2002, MNRAS, 335, 965
Zinnecker H., Bate M. R., 2002, in Crowther P. A., ed., ASP Conf. Ser. Vol. 267, Hot Star Workshop III: The Earliest Phases of Massive Star Birth. Astron. Soc. Pac., San Francisco, p. 209

APPENDIX A: NEGLECT OF BINARIES

In principle, 'hard' binary stars, either primordial or formed during core collapse through three-body processes, may play an important role in the cluster evolution. During gravitational encounters with single stars, a hard binary is likely to shrink, thus allowing the single star (possibly a former member of the binary if an exchange has occurred) to emerge with increased kinetic energy. Through this dynamical heating, hard binaries may suspend or even reverse core collapse (Heggie & Hut 2003, and references therein). Obviously, this might prevent the core from ever entering the high-density collisional phase needed in the runaway scenario. However, when the finite size of stars is taken into account in the numerical study of single–binary and binary–binary interactions, it appears that the collision of at least two of the stars is a likely event (see Fregeau et al. 2004 for the most recent cross-section computations and references about this question). Although using point-mass dynamics, Giersz & Spurzem (2003) studied the statistics of binary–single and binary–binary encounters occurring in their simulations of clusters containing primordial binaries and found that of the order of 50 per cent of these interactions should indeed lead to stellar mergers, for typical globular cluster parameters. It is therefore possible that binaries actually *foster* collisions rather than preventing them. This is exactly what was found in N-body simulations of relatively small clusters (most of them with $N_* \leqslant 131\,072$, one run with $N_* \simeq 585\,000$) by Portegies Zwart and collaborators (Portegies Zwart et al. 1999b; Portegies Zwart & McMillan 2002; Portegies Zwart et al. 2004). Furthermore, dissipative processes, such as collisions or tidal interactions, occurring during binary interactions may significantly reduce the heating effect of hard binaries, compared with the point-mass approximation (McMillan 1986; Goodman & Hernquist 1991; Chernoff & Huang 1996). To our knowledge, however, the impact of this on core collapse has not yet been studied explicitly.

Even if binaries probably do not prevent core collapse and collisions, it does not follow that they will not impede or modify the runaway process. Indeed, the cross-section for collision of a single star with a binary is of the order of $\pi GaM(V_{\rm rel}^{\infty})^{-2} \propto M$ where a is the binary semi-major axis and M the mass of the three stars, while it is approximately $\pi GRM(V_{\rm rel}^{\infty})^{-2} \propto M^{\alpha}$ with $\alpha \simeq 1.5$ for the collision with a single more massive star of mass M ($>50\,{\rm M}_{\odot}$) and radius R. According to mathematical modelling through the coagulation equation, runaway is expected only if the cross-section scales like M^{ζ} with $\zeta > 1$ (Lee 1993, 2000; Malyshkin & Goodman 2001).

This condition is not obeyed in the case of binaries competing with each other for interaction and merger with single stars. However, the coagulation equation is clearly at best a crude idealization for the complex stellar dynamical situation of interest here.

To simplify the problem, we have assumed in this work that no primordial binaries were present. We now examine if we are then justified to neglect binary process altogether consistently, in spite of the possibility of forming binaries dynamically. We do not consider binary formed by tidal interactions because their formation requires close passage at a distance of a few stellar radii at most. Their formation rate cannot then be significantly higher than collision rate and their post-capture evolution, though still a controversial issue, is likely to lead to merger anyway. We instead consider the question of binaries formed through (point-mass) three-body interactions.

The creation rate of such binaries is [Binney & Tremaine 1987, equation (8-7); see also appendix of Ivanova et al. 2005]

$$\dot{n}_{3b} \simeq C_{3b} n^3 \frac{G^5 M_*^5}{\sigma_v^9}, \tag{A1}$$

where n is the stellar number density and $C_{3b} \simeq 0.75$ (Goodman & Hut 1993; Heggie & Hut 2003).

We compare this with the collision rate,

$$\dot{n}_{coll} = n t_{coll}^{-1} \simeq 4\pi n^2 R_*^2 \left(1 + \frac{2GM_*}{R_*(V_{rel}^{\infty})^2}\right) V_{rel}^{\infty} \approx 8\pi \frac{n^2 G M_* R_*}{\sigma_v}. \tag{A2}$$

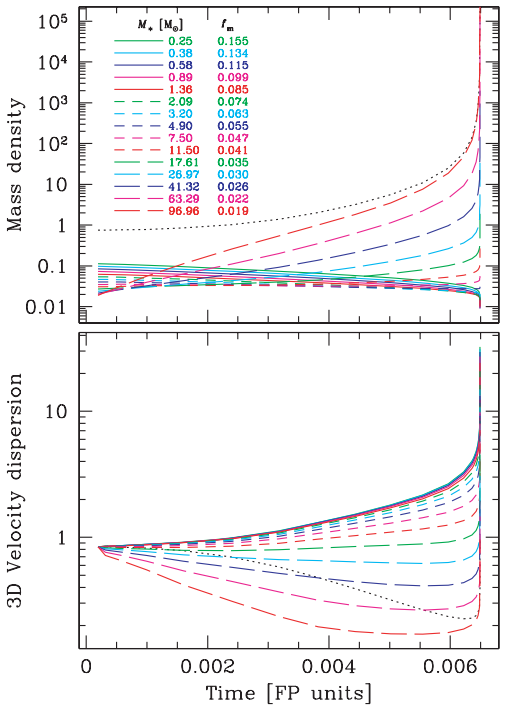

Figure A1. Core collapse of a $W_0 = 3$ King cluster with Salpeter mass function, computed with SPEDI. The mass spectrum is discretized into 15 components with the indicated individual stellar masses (m) and mass fraction (f_m). On the top panel, we represent the contribution of each mass component to the central mass density. The dotted line is the total density. The bottom panel shows the velocity dispersion of each component. The dotted line is the mass-averaged dispersion.

One gets

$$\frac{\dot{n}_{coll}}{\dot{n}_{3b}} \approx \frac{8\pi}{C_{3b}} \frac{R_* \sigma_v^8}{G^4 M_*^4 n} \approx \frac{500}{n R_*^3} \left(\frac{\sigma_v}{V_*}\right)^8 \tag{A3}$$

with $V_\odot = (2GM_\odot/R_\odot)^{1/2} = 618\,\mathrm{km\,s^{-1}}$. For typical 100-$M_\odot$ stars (dominating the central regions), $R_* \simeq 14\,R_\odot$, $V_* \simeq 1670\,\mathrm{km\,s^{-1}}$ and

$$\left.\frac{\dot{n}_{coll}}{\dot{n}_{3b}}\right|_{100\,M_\odot} \approx 7 \left(\frac{n}{10^6\,\mathrm{pc^{-3}}}\right)^{-1} \left(\frac{\sigma_v}{20\,\mathrm{km\,s^{-1}}}\right)^8. \tag{A4}$$

Thus, one cannot clearly exclude that the formation of three-body binaries will not compete with direct collision, at least for systems with a relatively low velocity dispersion.

Estimating a posteriori the central values of $\dot{n}_{3b}$ from MC runs is very difficult because of the steep dependences on n and σ_v, which make the estimate extremely noisy. Thus, to see how how $\dot{n}_{coll}$ and $\dot{n}_{3b}$ evolve during core collapse, we resort to the SPEDI gas-model code presented in Section 4.2.2. In Fig. A1, we follow the evolution of central densities and velocity dispersions in a 15-component SPEDI core-collapse simulation. Assuming $N_* = 10^6$ and $R_{NB} = 0.2\,\mathrm{pc}$, we can now compute what the central collision and three-body formation rates would have been during the core collapse. Because the evolution speeds up near the moment of core collapse, we use the central potential instead of time as independent variable in Fig. A2 where we plot the instantaneous and time-integrated rates for all mass components. For this size and star number, the cluster should

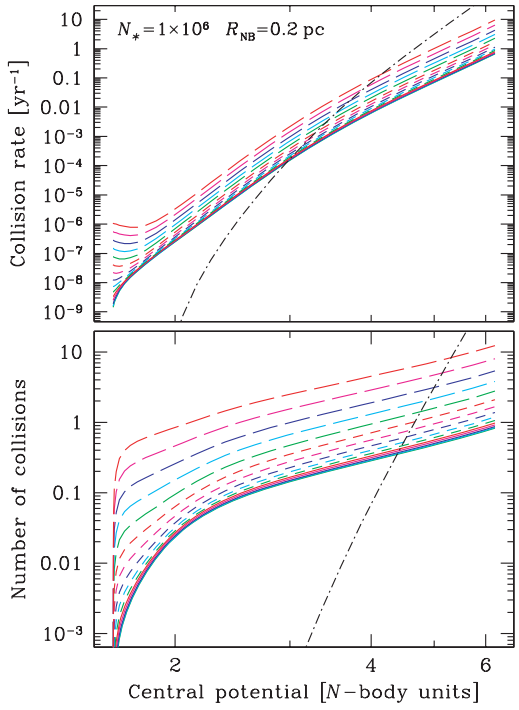

Figure A2. Same gaseous model simulation as on Fig. A1. Here we plot, for each mass component, the central collision rate per star (top panel) and integrated number of collision or collision probability (bottom panel) for a star near the centre. To avoid double counting, the rate for component i includes collisions with all components $j \leqslant i$. The steep (black) dash–dotted line is an estimate of the formation rate of three-body binaries (per star) obtained by using average stellar density and mass in equation (A1). Note that this simulation do not include the effects of collisions or binary formation but only two-body relaxation. Collision and binary formation rates have been estimated a posteriori assuming the cluster is made of 10^6 stars and its size is $R_{NB} = 0.2\,\mathrm{pc}$.

become collisional before the first binary forms. How this depends on the cluster parameters is expressed by either of the scalings

$$\frac{\dot{n}_{\rm coll}}{\dot{n}_{\rm 3b}} \propto {N_*}^3 R_{\rm cl}^{-1} \propto (\ln \Lambda\, T_{\rm rh})^{-2/3}\, {N_*}^{10/3} \tag{A5}$$

where $R_{\rm cl}$ is some characteristic cluster size (e.g. the half-mass radius). The strong dependence on N_* suggests that three-body binaries, which appear to dominate the collision process in N-body simulations may be of little importance in larger systems with $N_* \gtrsim 10^6$, such as very massive young clusters or proto-galactic nuclei. This analysis is in agreement with the results of Portegies Zwart et al. (2004) who find the dynamically formed binaries to play a lesser role in comparison with earlier, lower-N simulations (Portegies Zwart & McMillan 2002).

This paper has been typeset from a TEX/LATEX file prepared by the author.